



Master's Thesis

Origami Metamaterials automatic design

Hugo Penichou

Supervised by Professor Selman Sakar and Professor Renee Zhao

Contents

1	introduction	4
1.1	Context and motivation	4
1.2	Problem Statement	5
1.3	Objective and Scope	5
2	Background and Literature Review	6
2.1	Origami patterns: a natural occurring phenomena	6
2.1.1	Origami Patterns in Living Organisms	6
2.1.2	Spontaneous Emergence of Origami Patterns in Engineering Structures	7
2.1.3	Buckling of Thin Structures and Origami-Based Solutions	8
2.2	Origami in Engineering	9
2.3	Manufacturing of origami structures	12
2.3.1	MultiMaterial 3D printed approach	12
2.3.2	Monomaterial 3D printer	13
2.4	Origami and Mechanical Metamaterials	14
2.5	Simulation Methods	14
2.6	Crease Types	15
2.6.1	Curved Creases for Post-Buckling Shape Control	16
3	Methods and Materials	17
3.1	Preliminary Work Based on Past Research at Zhao’s Lab	17
3.1.1	Compression and Torsion Applied to Mylar Foils	17
3.1.2	Introduction of pre-creases in mylar cylinder	18
3.1.3	Exploring Reinforcement Strategies on Mylar	20
3.1.4	Conclusion of Preliminary Work	21
3.2	Design of Origami Patterns Using Parametric Code	21
3.2.1	Parametric CAD Code with Fusion 360	23
3.2.2	Yoshimura Pattern	24
3.2.3	Kresling Pattern	25
3.3	Computational methods	26
3.3.1	Simulation of the Complete Mechanism	26
3.3.2	Design and simulation of living hinges	28
3.4	Semi-analytical Method	31
3.4.1	Finite Element Formulation of Bar Elements	31
3.4.2	Symmetric Tangent Stiffness Matrix Expansion	32
3.4.3	Rotational Spring Elements	33
3.4.4	Dihedral Angle and Vector Definitions	34
3.4.5	Simulation Testing of Origami Materials	34
3.5	3D Printing of Origami Metamaterials	35
4	Results and Discussion	37
4.1	Full Pipeline	37
4.2	Playing with Multiple Designs	38
4.3	The Choice of the Panel Interface	40
4.4	Manufacturing	41
4.5	Potential for Improvements	43
4.5.1	AI-Assisted Design Tools	43
4.5.2	Expanding to Other Origami Patterns	44

4.5.3	Enhancing the User Experience	44
4.5.4	Enhanced Simulation and Validation	45
4.5.5	Manufacturing Integration and Material Considerations	45
4.5.6	Collaborative Research Platform	45

Abstract

Origami, originating from the traditional Japanese art of paper folding, enables the creation of intricate structures through precise folding techniques. In engineering, an ideal origami-inspired material consists of rigid panels interconnected by creases that facilitate controlled deformation. Over the past century, origami principles have evolved from an artistic discipline to a foundation for advanced engineering applications.

Origami-based designs now play a crucial role in deployable structures, shape-morphing materials, energy absorbers, and mechanical metamaterials whose properties are dictated primarily by their geometry rather than their composition.

Traditional fabrication of origami structures often involves manual folding or the creation of pre-defined creases in thin sheets, a process that is labor-intensive, time-consuming, and limited in complexity. Recent advances in additive manufacturing, particularly stereolithography (SLA) 3D printing, enable the rapid and cost-effective fabrication of intricate origami geometries.

This thesis presents an integrated pipeline for the generative design, simulation, and fabrication of origami metamaterials. The workflow leverages parametric modeling, finite element and semi-analytical simulations, and resin-based 3D printing to accelerate the development of programmable, foldable mechanical systems. It further demonstrates how crease design—ranging from straight folds to elastica-inspired curves and living hinges—controls folding predictability, stress localization, and energy absorption.

Keywords: Origami metamaterials, SLA 3D printing, Deployable structures, Bistability, Programmable mechanics.

1 introduction

1.1 Context and motivation

My research was conducted in the Zhao Lab at Stanford University, a laboratory dedicated to the discovery and development of advanced metamaterials, with a strong focus on structural mechanics and mechanical metamaterials. In addition to its core work in material science, the Zhao Lab is actively engaged in biomedical applications, particularly the development of spinner robots for minimally invasive treatments of blood clots.

Despite the wide range of projects within the lab, origami-based design principles consistently prove to be a powerful tool for engineering novel structures. A prime example is the spinner robot, which is based on the Kresling origami pattern. This pattern offers unique mechanical properties, including a helicoidal geometry capable of generating thrust when rotating, and an intrinsic ability to undergo axial contraction. These features can be strategically leveraged for biomedical purposes, such as capturing blood clot debris or delivering drugs to precise locations within the body.

The current manufacturing process for spinner robots begins with cutting thin plastic sheets using a vinyl cutter, followed by manual folding and gluing to form the final structure. This method is currently suitable for producing relatively large spinner robots, approximately 1 cm in diameter, designed to navigate regions such as the digestive tract, where they deliver drugs under the guidance of an external magnetic field. However, when scaling down the spinner robots for vascular applications, this approach reaches its limitations. For smaller-scale devices,

the Kresling structure has been fabricated using high-resolution stereolithography (SLA) 3D printing. While this allows miniaturization and the retention of the general Kresling-inspired geometry, the printed devices lose the shape-changing capabilities intrinsic to traditional, crease-based Kresling origami.

Beyond medical applications, the Zhao Lab is also at the forefront of developing magnetic metamaterials. Although not strictly based on origami, these structures draw inspiration from kirigami patterns. The key distinction lies in the fabrication method: rather than relying on creases to create hinges, kirigami introduces strategic cuts into the material, resulting in flexible sections capable of controlled folding. These magnetic metamaterials are typically fabricated by molding resin infused with magnetic particles, such as neodymium-iron-boron (NdFeB) powder, enabling the structures to deform or reconfigure when exposed to an external magnetic field.

1.2 Problem Statement

Origami metamaterials are structures capable of folding and transforming their geometry, often exhibiting unique mechanical properties such as directional stiffness, bistability, or energy absorption. These properties are primarily dictated by the specific origami pattern implemented in the design. Beyond the choice of pattern, an essential challenge lies in programming the material itself to ensure that the desired folding behavior reliably emerges during deployment. This requires the strategic incorporation of creases, reinforcements, or local material modifications to guide the folding process and achieve predictable, functional configurations.

1.3 Objective and Scope

The objective of this project is to establish a complete, accessible pipeline for the design, simulation, and prototyping of programmable origami metamaterials. The central goal is to enable the embedding of predefined crease patterns into materials, such that specific, predictable folding behaviors emerge when the structure is deployed.

We focus exclusively on **origami**, not **kirigami**, in this study. Although the two are mechanically similar—both rely on introducing **imperfections to guide folding behavior**—the methods by which these imperfections are introduced differ significantly. In origami, folds are directed through pre-creased lines or regions of varying material stiffness. In contrast, kirigami introduces cuts or holes along specific lines to locally alter stiffness and enable complex deformation. While kirigami offers additional geometric flexibility, origami has the distinct advantage of preserving material continuity. This feature makes it particularly suitable for applications that require air tightness or structural integrity, such as pneumatic actuators or deployable space structures. For these reasons, the scope of this master's thesis is limited to origami-based strategies, excluding kirigami approaches.

The proposed workflow consists of three main stages for each design iteration

1. **Generative Design:** Creation of crease patterns and corresponding geometries using parametric tools to facilitate rapid exploration of multiple design variations.
2. **Simulation:** Numerical validation of the folding behavior using Finite Element Analysis (FEA) and simplified wire frame models to predict structural responses and performance.
3. **Fabrication and Testing:** Production of physical prototypes, primarily through 3D printing, followed by experimental testing to evaluate the effectiveness of the design.

The ultimate aim is to deliver an **open-source toolkit** that enables researchers and practitioners to easily experiment with and prototype origami meta materials. By adopting a parametric and modular approach, the framework allows users to apply crease maps to a wide range of shapes and rapidly assess their performance.

2 Background and Literature Review

To gain a deeper understanding of origami structures, we conducted a literature review that revealed key insights discussed in the sections below:

- **Origami in Nature and Engineering:** Naturally occurring folding patterns in biological systems and their influence on the development of engineered origami structures.
- **Mechanical Frameworks:** Theoretical models used to describe and exploit the mechanical behavior of origami for creating functional materials and deployable structures.
- **Fabrication Techniques:** Recent advances in manufacturing methods addressing current limitations and enabling more practical applications of origami-based systems.
- **Simulation Approaches:** Mathematical and computational tools used to model and predict the behavior of origami under various loading conditions.

2.1 Origami patterns: a natural occurring phenomena

Origami-inspired structures are not limited to artificial designs but can also be observed in nature and in the spontaneous deformation of engineered structures.

2.1.1 Origami Patterns in Living Organisms

Nature has evolved sophisticated folding mechanisms that parallel engineered origami systems, demonstrating the fundamental efficiency of controlled deployment strategies across biological scales. These naturally occurring crease patterns enable predetermined deployment sequences that transform compact, folded configurations into functional extended structures with remarkable precision and speed.

Plant leaves exemplify this principle through their development from tightly packed buds to fully deployed photosynthetic surfaces. During budding, leaves must achieve maximum compactness within the confined space of protective bud scales while maintaining the structural integrity necessary for rapid deployment when environmental conditions become favorable. The folding patterns observed in deciduous tree leaves during this process can be described as sophisticated variations of the Miura-ori pattern, utilizing alternating mountain and valley folds to achieve efficient packing ratios [5].

Insect wing deployment represents another remarkable example of biological origami engineering. The wings of beetles such as Chrysomelidae demonstrate complex folding mechanisms where thin, delicate membranes achieve extraordinary compaction ratios while maintaining the ability to deploy rapidly for flight. These wings employ hierarchical folding strategies that combine radial and transverse creases, enabling the wing membrane to fold to a fraction of its deployed size beneath rigid wing covers (elytra). Upon deployment, the stored elastic energy in the crease

lines facilitates rapid unfolding, demonstrating the dual role of origami patterns in both storage efficiency and actuation [5].

These biological systems illustrate fundamental design principles that have informed engineering applications: the use of pre-programmed crease patterns to control deployment sequences, the integration of structural and actuation functions within folding mechanisms, and the achievement of high packing ratios without compromising structural performance in the deployed state.

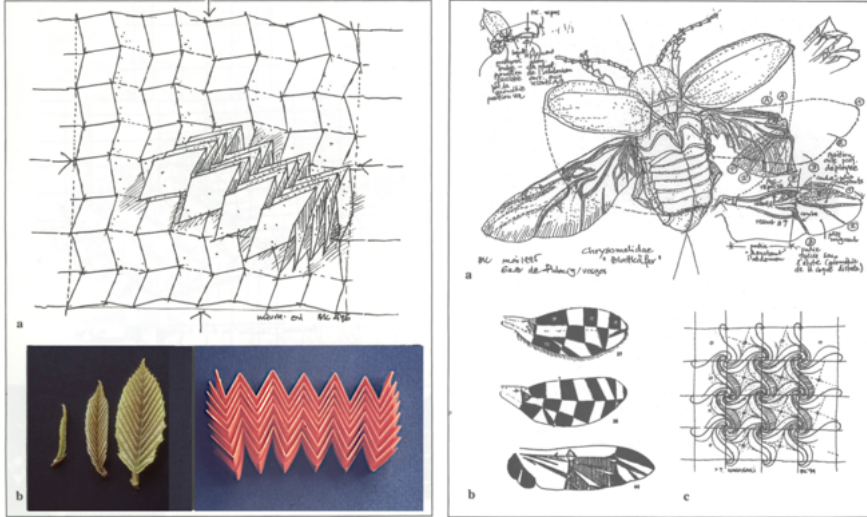


Figure 1: Kresling CAD construction showing unit facets and geometric assembly.

Figure 2: Origami inspired shape naturally occurring in the leaves of the deciduous tree and the wings of the Chrysomelidae. Schematic obtained from this paper: [5]

2.1.2 Spontaneous Emergence of Origami Patterns in Engineering Structures

The discovery of fundamental origami patterns through structural analysis represents a paradigm shift in understanding the relationship between geometric instability and functional design. Rather than being intentionally designed, many of the most influential origami patterns in engineering emerged from careful observation of failure modes in thin-walled structures, revealing that nature's geometric solutions can manifest spontaneously under mechanical loading.

The **Yoshimura pattern** exemplifies this phenomenon, having been first identified by Yoshimura during systematic studies of axial compression in thin cylindrical shells [12]. When subjected to compressive loads exceeding the classical buckling threshold, these shells spontaneously reorganize into a characteristic diamond-faceted geometry featuring alternating mountain and valley folds arranged around the cylinder circumference. This post-buckling configuration represents a stable equilibrium state that efficiently redistributes stress concentrations while maintaining structural integrity, effectively transforming what was traditionally considered structural failure into a controlled deformation mode.

The geometric characteristics of the Yoshimura pattern—diamond-shaped facets with specific angle relationships and fold line orientations—arise directly from the energy minimization principles governing thin-shell mechanics. The pattern's emergence demonstrates how geometric constraints

and material properties can spontaneously generate complex three-dimensional structures from initially uniform cylindrical geometries.

Similarly, the **Kresling pattern** was discovered through analysis of thin-walled cylinders under combined torsional and axial loading conditions [6]. This loading scenario produces a distinctive helical folding geometry that integrates twisting and compression deformation modes. The resulting structure exhibits remarkable mechanical properties, including progressive collapse behavior, energy absorption capacity, and reversible deployment characteristics. The Kresling pattern's ability to couple rotational and translational motion through geometric constraints has made it particularly valuable for applications requiring controlled deployment, shock absorption, and mechanical energy storage.

These discoveries fundamentally altered the engineering perspective on structural instability, transforming buckling from an undesirable failure mode into a design tool for creating functional, deployable structures. The spontaneous emergence of these patterns under loading demonstrates that origami-like geometries represent natural solutions to mechanical optimization problems, providing a foundation for intentionally designed origami-inspired engineering systems.

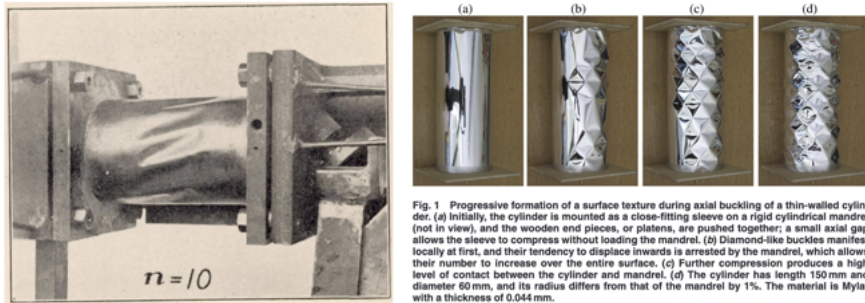


Figure 3: Kresling CAD construction showing unit facets and geometric assembly.

Figure 4: On the left: Kresling patterns emerging spontaneously in the torsional buckling of a metal cylindrical shell obtain from [3]. On the right: Yoshimura patterns emerging naturally from the controlled compression of a mylar cylindrical shell obtained from: [4]

2.1.3 Buckling of Thin Structures and Origami-Based Solutions

Thin-shell structures are extensively used in aerospace applications due to their exceptional strength-to-weight ratio, including fuel tanks, pressure vessels, and architectural components. However, these structures suffer from extreme sensitivity to geometric imperfections, causing unpredictable buckling at loads significantly below theoretical predictions. Wang et al. [11] quantify this through the **Knock-Down Factor (KDF)**—the ratio of measured to theoretical buckling loads. NASA typically requires conservative **KDF** values of 0.3–0.4, necessitating substantial safety margins that increase structural weight and cost. The authors demonstrate that improved manufacturing tolerances and imperfection-aware models can increase **KDF** values to 0.886, enabling lighter designs.

Origami engineering offers a transformative approach to this challenge. By intentionally introducing **pre-defined crease patterns** such as the elastica creases into thin shells, engineers can

guide and control the buckling process. This approach enhances predictability while enabling structures that fold controllably opening the door to energy storing devices by storing energy thought the folding and streaching of the creases, as well as shock absorbing devices where enegry in stored in the plastic controlled compression of the origami structure [7].

2.2 Origami in Engineering

This paper provides a comprehensive survey on origami engineering methods and principles [9]. Origami engineering leverages geometric folding concepts to create functional, reconfigurable, and often multifunctional structures for a broad range of applications. In essence, the paper highlights the following key features of origami engineering:

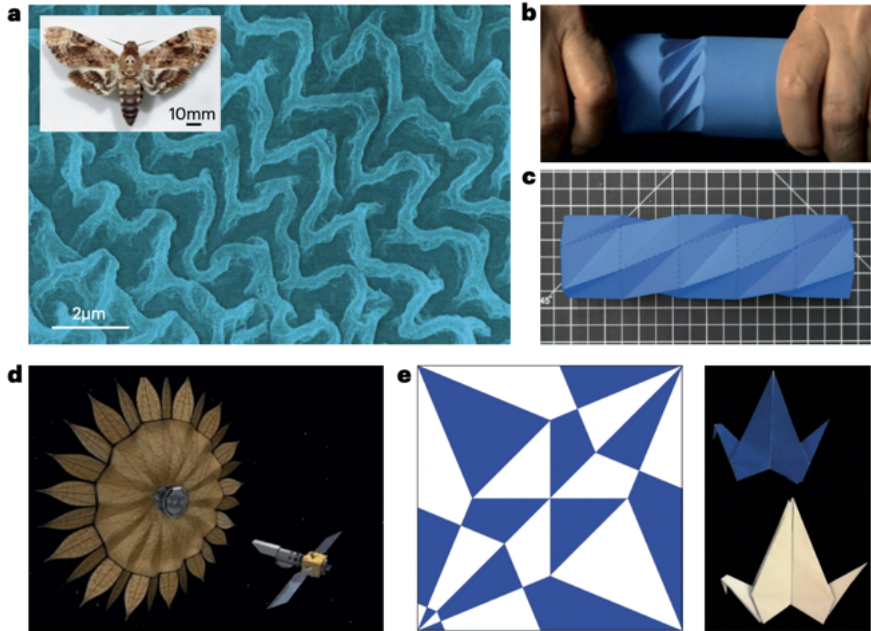


Figure 5: Illustrative examples of origami principles across nature, spontaneous mechanics, and engineered systems. (a) Folding in nature, exemplified by the Hawkmoth wing structure. (b) Spontaneous emergence of a Kresling-like pattern when a thin cylindrical paper shell is twisted. (c) Engineering a Kresling unit cell by pre-folding a flat sheet of paper along specific crease lines. (d) Application of origami in advanced engineering concepts such as NASA’s Starshade project—designed as a large deployable structure to block starlight and enhance the observation of exoplanets. (e) A crease map encoding the mountain and valley folds required to obtain a desired 3D geometry from a flat sheet. Images adapted from [9].

Fundamental Characteristics of Origami Structures:

- Developability: The ability of a structure to fold from a flat sheet into a 3D shape without stretching or tearing. Developable origami undergoes nearly isometric transformations, ideal for thin-sheet structures like Miura-ori or Hylar patterns.

- Flat Foldability: The capability of an origami structure to return to a fully flat state. Flat foldability is a distinct property from developability and often desirable for compact storage or transport (e.g., Kresling tubes, Eggbox patterns).
- Rigid Foldability: Refers to folding transformations where panels remain undeformed, with all deformations concentrated along crease lines. This property is crucial when using stiff materials like metals or composites.
- Thick Origami Models: In real engineering applications, panel thickness must be considered. Various strategies such as tapered panels, offset hinges, or kirigami techniques are employed to accommodate thickness while preserving foldability.

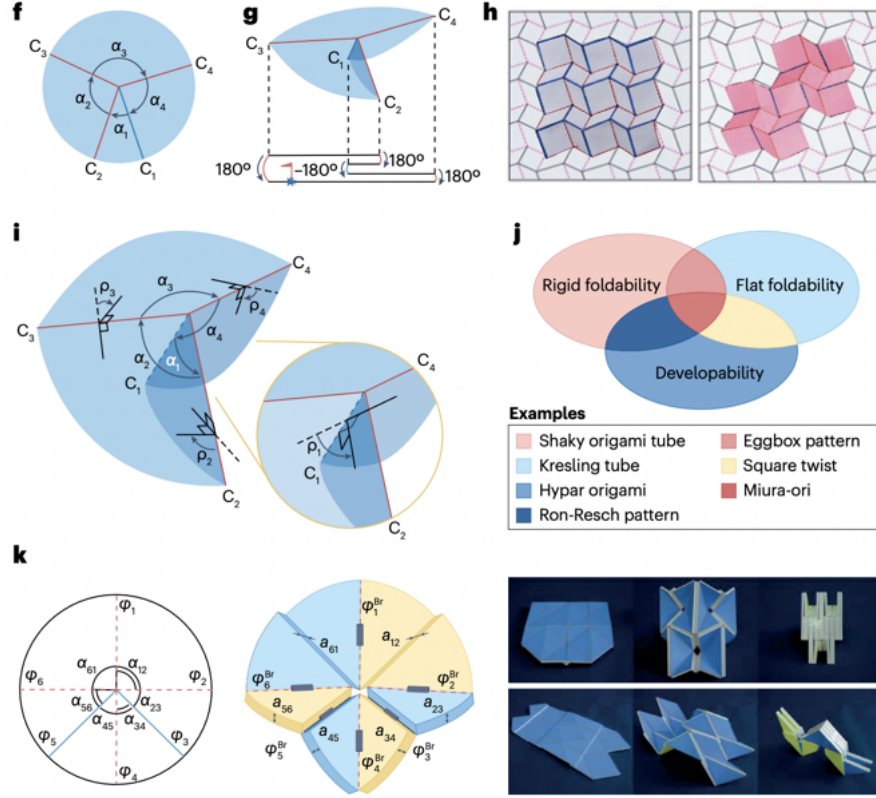


Figure 6: Overview of a theoretical framework to integrate origami in engineering. (f) A degree-four origami vertex in its developed (unfolded) state. (g) Folded configuration of the same degree-four vertex, illustrating the flat foldability condition. (h) Examples of single-vertex crease layouts showing mountain folds (thick blue lines) and valley folds (dashed red lines): square twist (left) and Mars pattern (right). (i) Turning angles between panels used to evaluate rigid foldability, based on the Belcastro-Hull condition. (j) Venn diagram of foldability concepts: flat foldability, developability, and rigid foldability, with associated examples. (k) Illustration of thickness-accommodating origami using the offset hinge technique on a waterbomb pattern. Symbols: α_i are panel angles, φ_i are crease angles, C_i are individual creases, ρ_i are turning angles, and Br refers to Bricard linkages. Images adapted from [9], with parts a and d courtesy of L. T. Wasserthal and NASA/JPL, respectively; part k reprinted with permission from Ref. 17 (AAAS).

Manufacturing Methods

The paper reviews several fabrication approaches for origami structures, including:

- Paper and Polymer-Based Models: Fast, low-cost prototyping using craft paper, polyester films, or composite sheets, often combined with laser cutting for precise crease definition.
- CNC-Milled Models: High-precision cutting of panels and hinges from polymer or metal sheets, enabling the fabrication of multistable, mechanically tunable origami.
- CNC-Milled Models: High-precision cutting of panels and hinges from polymer or metal sheets, enabling the fabrication of multistable, mechanically tunable origami..

- **Folding and Assembly:** Essential for both developable and non-developable patterns, where accurate folding and joining of components are required to achieve the desired structure.

Experimental Testing and Characterization:

Performance testing of origami structures involves:

- **Custom Experimental Set-ups:** Due to their large deformations and non-linear behavior, specialized fixtures (e.g., Saint-Venant set-up) are used to prevent unwanted constraints during mechanical testing.
- **Data Collection:** Load-displacement curves, deformation tracking via high-resolution cameras, and digital image correlation methods are employed to evaluate mechanical performance.
- **Actuation:** Origami structures can be actuated using pneumatic, magnetic, or stimuli-responsive (4D printing) methods, enabling shape morphing or self-deployment.

Conclusion: Origami engineering provides a rich design space to create reconfigurable, multifunctional structures. Its core advantages lie in the interplay between geometry, material selection, and precise fabrication methods, enabling applications in metamaterials, robotics, deployable structures, and medical devices.

2.3 Manufacturing of origami structures

2.3.1 MultiMaterial 3D printed approach

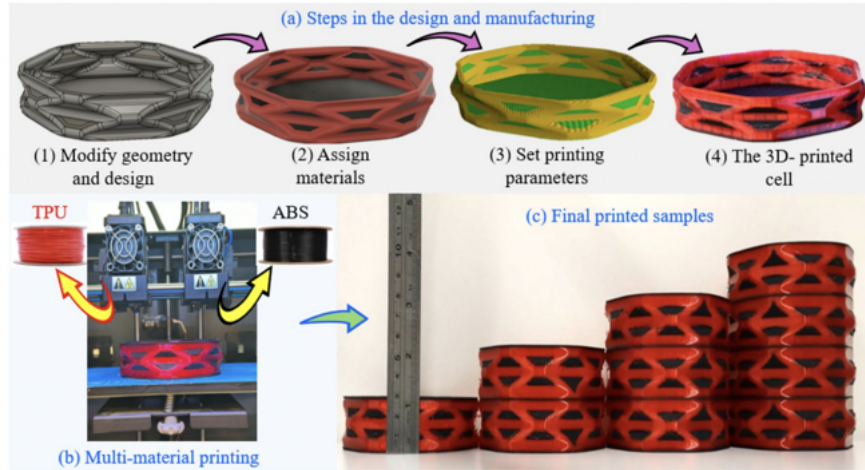


Figure 7: Fabrication steps of a dual-material 3D-printed Yoshimura cylinder. The structure integrates two types of materials: the hinges are printed using an elastomeric filament (TPU – Thermoplastic Polyurethane), providing flexibility at the folds, while the rigid panels are printed with a stiff thermoplastic such as ABS (Acrylonitrile Butadiene Styrene). This material combination allows for controlled folding behavior and repeatable deployment. Image adapted from [1].

In the following study, a novel manufacturing approach for origami-inspired structures was introduced using a multi-material additive manufacturing (MMAM) process [1]. The focus of the study lies in structures for high-end applications such as deployable systems for space, including solar panels, antennas, masts, and compartments. The authors emphasize that conventional manufacturing methods often limit the practical implementation of such structures due to challenges in fabricating complex geometries with controlled foldability. To overcome these limitations, MMAM was employed, offering the possibility to fabricate structures with localized variations in stiffness, enabling the integration of functional crease lines. In this work, the authors produced cylindrical structures with embedded Yoshimura origami patterns using a dual-extrusion 3D printer. Thermoplastic polyurethane (TPU) was used to form the flexible crease regions, while acrylonitrile butadiene styrene (ABS) provided the rigidity required for the panel regions. Cyclic compression tests were performed on these multi-material cylinders to assess their foldability and mechanical integrity. The results showed no significant failure along the bi-material interfaces at the crease lines within single-cell structures, demonstrating the potential of MMAM for manufacturing deployable origami-inspired systems.

2.3.2 Monomaterial 3D printer

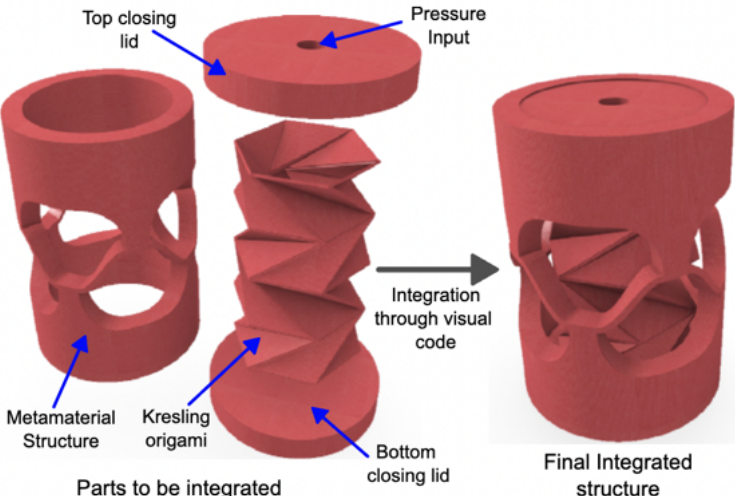


Figure 8: Pneumatic actuator based on the Kresling origami pattern, fabricated using a single-material 3D printer. This approach eliminates the need for dual-extrusion or multi-material printers, significantly improving accessibility and scalability of fabrication. The actuator harnesses the geometric properties of the Kresling pattern for reversible deformation under pressure. Image adapted from [2].

De Souza Oliveira et al. [2] demonstrate the fabrication of an inflatable origami actuator using standard FDM 3D printing with TPU, requiring no specialized equipment. Their method enables the monolithic integration of a Kresling-based origami structure with a metamaterial shell, avoiding manual assembly and enhancing structural integrity. A Grasshopper-based parametric design tool facilitates rapid geometry adjustments, streamlining the design process. However,

limitations remain. The FDM process constrains resolution, particularly for fine folds, and requires extremely low print speeds, reducing scalability. Additionally, sealing the inflatable cavity still involves manual Ecoflex coating, introducing potential leakage risks. Overall, the method offers a simple and robust fabrication route, but precision and scalability challenges persist.

2.4 Origami and Mechanical Metamaterials

As described in [13], mechanical metamaterials are artificially engineered materials that exhibit unconventional mechanical properties—such as tunable stiffness, programmable shape morphing, and unusual Poisson ratios. A prominent design strategy relies on **“origami-based metamaterials”**, which are created by introducing crease patterns into thin sheets to enable controlled folding.

These structures are typically composed of rigid panels connected by flexible creases. To ensure predictable mechanical behavior, the panels must be significantly stiffer than the creases. The overall deformation of such structures is governed by the *mechanical energy landscape*, which characterizes how elastic energy varies throughout the folding process. This landscape plays a central role in determining deployability, stability, and stiffness.

Origami metamaterials are generally categorized into two types:

- **Rigid origami:** Only the creases deform and store energy, while the panels remain undeformed. This results in predictable kinematics and is especially suited for applications in shape morphing. A notable example is the Miura pattern, which offers a single degree of freedom.
- **Deformable origami:** Both creases and panels undergo deformation and store elastic energy, leading to a more complex mechanical response. Patterns such as Kresling, Yoshimura, and curved origami often exhibit panel bending and buckling, enabling properties like bistability, tunable stiffness, and coupled deformation.

Origami metamaterials find applications across diverse fields, including soft robotics, deployable structures, flexible electronics, and medical devices. Their mechanical behavior is programmed not by the material itself, but by the geometry and topology of the folding pattern. This makes them highly versatile tools for designing structures with tailored mechanical responses.

2.5 Simulation Methods

To simulate and predict the deformation and stress distribution in origami structures, we explored various approaches in the literature. A commonly used method in structural mechanics is Finite Element Analysis (FEA). While FEA is highly versatile, it is also computationally intensive and requires careful setup, including appropriate mesh generation and the choice of suitable element types.

In an effort to find more origami-specific and computationally efficient alternatives, we reviewed literature focused on reduced-order or energy-based methods. One particularly relevant approach is presented in Schenk and Guest’s work [10], which models origami as a network of panels connected by creases, incorporating bending, folding, and stretching behaviors.

In this model:

- **Bars** along panel edges are allowed to stretch, contributing axial strain energy.
- **Creases** are modeled as torsional springs, introducing rotational stiffness at the fold lines.
- **Panel bending**, especially in quadrilateral panels, is represented by additional bending springs across diagonal crease lines.

The simulation minimizes the total deformation energy of the structure at each step. Equilibrium is reached when the first derivative of the total strain energy with respect to nodal displacements is zero, corresponding to a stable mechanical configuration.

This method offers a physically intuitive and computationally lighter alternative to traditional FEA, especially well-suited for studying the nonlinear mechanics of non-rigid origami.

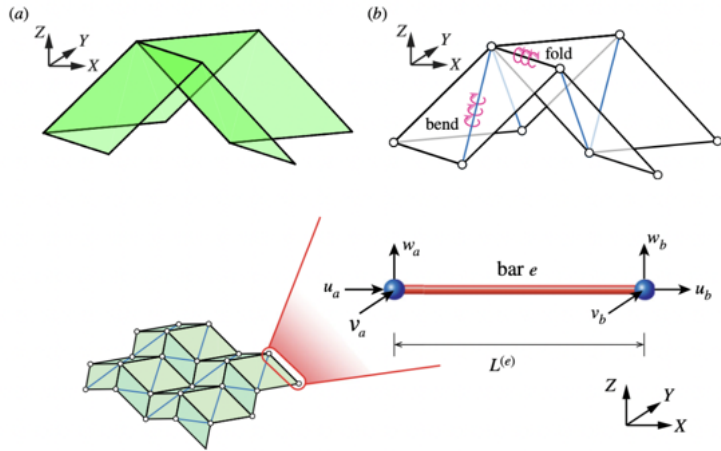


Figure 9: Illustration of the primary sources of elastic energy in the deformation of an origami metamaterial. Strain energy arises in the bar elements (e.g., panel edges), while torsional strain is concentrated around fold elements along crease and bend lines. The figure depicts a Miura-ori pattern, but the same principles apply to Kresling and Yoshimura patterns—with the exception of bend lines, which are generally not considered in triangular panel configurations [8].

2.6 Crease Types

In origami engineering, complex folding patterns are typically described using crease maps—planar diagrams that indicate the positions and orientations of folds to be applied to a flat sheet. These maps specify the locations of mountain and valley folds, enabling the transformation of a 2D surface into a 3D structure with tailored mechanical properties.

Several canonical crease patterns have been extensively studied due to their geometric elegance and favorable mechanical behavior:

- **Miura-ori:** A tessellated pattern of parallelograms enabling rigid-foldable structures with negative Poisson’s ratio and high compactness, originally developed for space applications.
- **Yoshimura pattern:** Emerges naturally from axial buckling in cylindrical shells, forming a diamond-like configuration of alternating creases that efficiently redistributes stress.

- **Kresling pattern:** Combines helical and radial creases, yielding a twist-folding motion often used in deployable and energy-absorbing structures.
- **Waterbomb base:** A radial fold pattern enabling bistable and reconfigurable geometries, frequently used in origami actuators and soft robotics.
- **Eggbox pattern:** An alternating grid of mountain and valley folds with tunable stiffness, capable of achieving volumetric contraction and expansion.
- **Tachi-Miura polyhedron (TMP):** A three-dimensional extension of Miura-ori with a curved surface, useful in morphing structures and architectural applications.

These foundational patterns form the building blocks for more complex systems and can be combined or modified to tailor mechanical response.

2.6.1 Curved Creases for Post-Buckling Shape Control

In addition to traditional straight-crease designs, curved-crease origami introduces new degrees of freedom for controlling post-buckling shapes. In their study, Lee et al. [7] present a novel approach for post-buckling shape control in thin-walled cylindrical shells by embedding pre-designed curved creases. This method exploits the imperfection sensitivity of shells under axial compression to guide deformation into predictable and programmable configurations.

By incorporating elastica-inspired curved creases, local bending stiffness is strategically reduced along targeted fold lines. These engineered imperfections act as deformation triggers, steering the structure from an unstable tubular form into a well-defined, stable buckled configuration.

Compared to straight-crease patterns, the curved-crease design offers:

- Greater precision in controlling post-buckling geometry,
- Access to lower-energy deformed states through favorable stress redistribution,
- Bistability, enabling potential applications in energy absorption, deployable systems, and shape-morphing structures.

This strategy highlights a growing trend in origami-inspired mechanics: leveraging geometric constraints to transform structural instability into functional advantage.

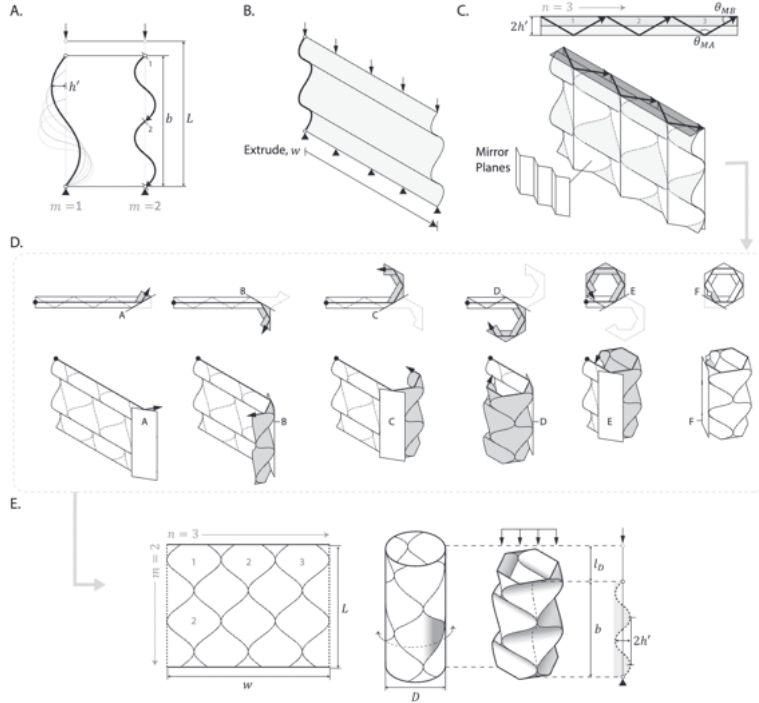


Figure 10: Schematic from [7] illustrating the fabrication of an origami cylinder using curved creases instead of conventional straight ones, as typically found in Yoshimura and Kresling patterns.

3 Methods and Materials

3.1 Preliminary Work Based on Past Research at Zhao's Lab

The initial objective of this research was to investigate the spontaneous emergence of origami patterns in thin cylindrical shells subjected to axial compression and torsional loads. This approach draws inspiration from classical observations where specific deformation modes—such as the Yoshimura diamond pattern and the Kresling twist pattern—naturally emerge in thin-walled structures under stress.

3.1.1 Compression and Torsion Applied to Mylar Foils

To test this concept, thin Mylar sheets were laser-cut into uniform rectangular strips and wrapped around a cylindrical clutch. The clutch was mounted on an Instron mechanical testing machine to apply controlled compressive loads. The hypothesis was that post-buckling behavior under sufficient loading would lead to the formation of structured origami patterns.

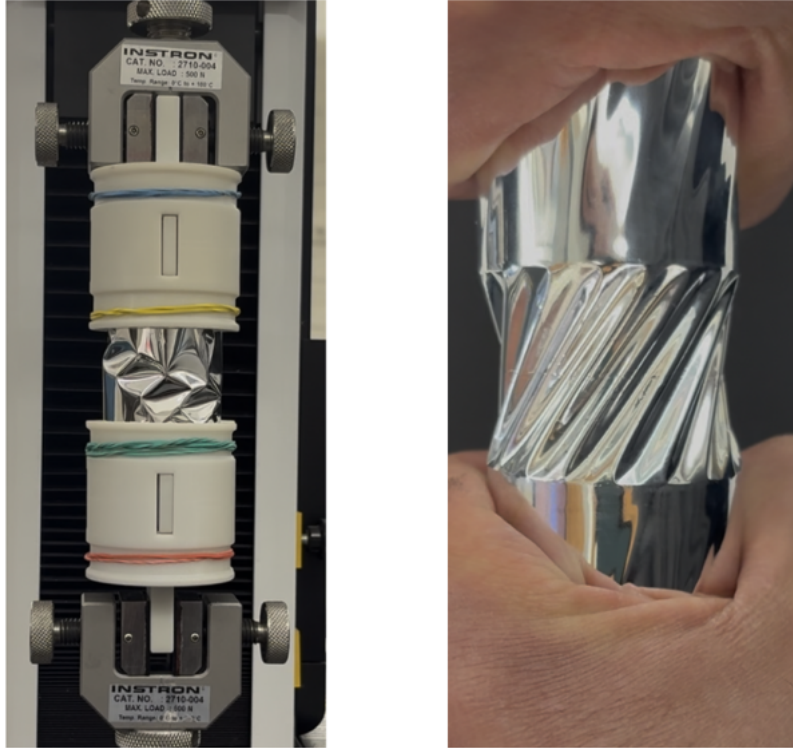


Figure 11: Kresling CAD construction showing unit facets and geometric assembly.

Figure 12: Compression of a cylinder wrap Mylar foil with a pre-crease introduce of the horizontal axis

As discussed by Wang et al. [11], thin-walled cylinders are highly sensitive to geometric imperfections. To leverage this sensitivity and promote controlled buckling, we explored two main strategies:

1. Introducing **pre-creases** via manual scoring or localized heating.
2. Adding **reinforcement structures** to locally modulate stiffness and guide deformation.

3.1.2 Introduction of pre-creases in mylar cylinder

To ensure repeatability, all samples were laser-cut to standardized dimensions. Pre-creases were applied at predefined positions inspired by classical crease maps. Samples were wrapped around custom cylindrical mandrels fabricated using high-resolution SLA 3D printing, ensuring tight and uniform contact during loading.

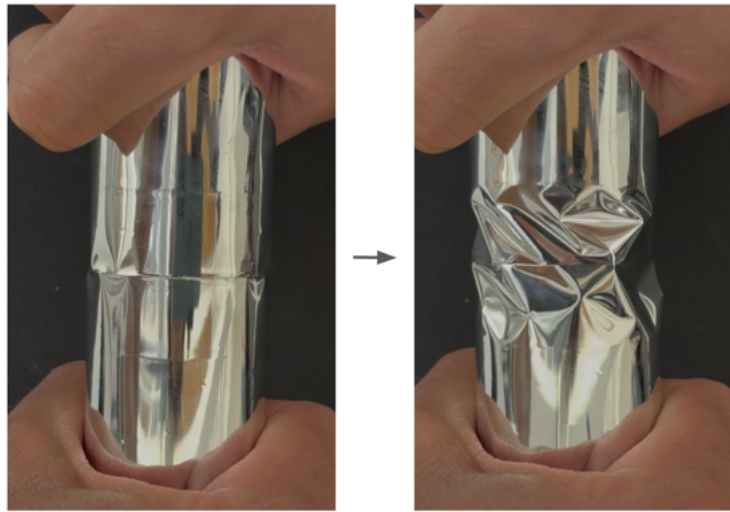


Figure 13: Kresling CAD construction showing unit facets and geometric assembly.

Figure 14: Compression of a cylinder wrap Mylar foil with a pre-crease introduce of the horizontal axis

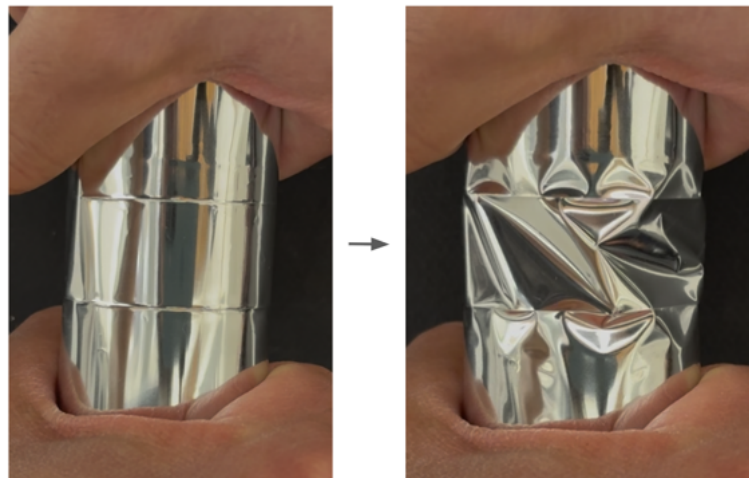


Figure 15: Kresling CAD construction showing unit facets and geometric assembly.

Figure 16: Compression of a cylinder wrap Mylar foil with two horizontal pre-crease

Despite multiple trials, these tests did not consistently produce well-formed or localized origami patterns. The observed buckling was often erratic and failed to organize into recognizable geometric modes. Several factors may have contributed to these results:

- The pre-creases may not have generated sufficient stiffness contrast to meaningfully influ-

ence the deformation energy landscape.

- The bending stiffness of Mylar, while relatively low, remains higher than that of common origami materials such as paper or polymer membranes, likely inhibiting pattern localization.

3.1.3 Exploring Reinforcement Strategies on Mylar

As an alternative to pre-creasing, we investigated the possibility of guiding deformation by locally reinforcing the Mylar surface. However, Mylar's inherently non-adhesive properties posed a significant challenge. Our initial approach involved applying paint as a stiffening layer, which ultimately failed due to:

- Poor adhesion, resulting in flaking and easy removal.
- The need for thick paint layers to significantly affect stiffness, which were difficult to apply uniformly.



Figure 17: Attempted reinforcement of Mylar using a painted coating. Poor adhesion and non-uniformity limited its effectiveness.

To overcome these issues, we explored bonding separate reinforcement structures onto the Mylar foil. This approach raised two main challenges:

1. How to fabricate suitable reinforcement structures.
2. How to reliably bond them to the Mylar surface.

Our first attempt involved 3D printing the reinforcement elements using an FDM printer. However, the printed features were limited by the minimum layer height, making them too bulky and imprecise for fine crease control.

We then moved to laser-cut polymer films to produce thin, precisely shaped reinforcement layers. While this method allowed high geometric fidelity, bonding remained problematic. We tested various adhesives available in the lab, including:

- **Cyanoacrylate and epoxy** glues: showed virtually no adhesion to the Mylar surface.

- **UV-curable glue:** offered slightly better adhesion but required transparent reinforcement films to allow light penetration for curing, making the method unreliable and limiting material choices.

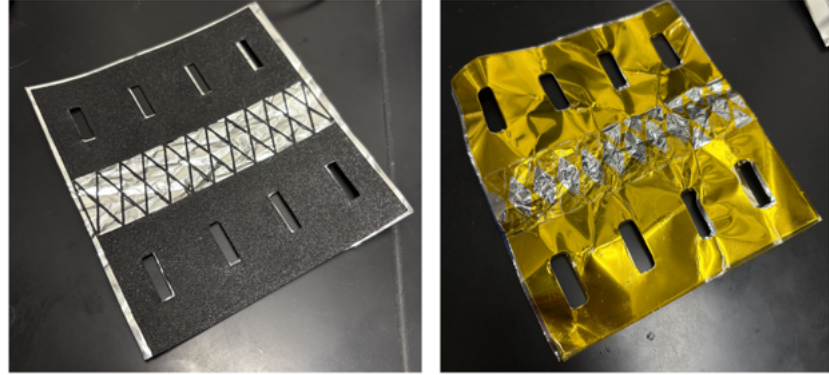


Figure 18: Kresling CAD construction showing unit facets and geometric assembly.

Figure 19: Explored methods for reinforcing Mylar using external structures. Adhesion remained the key challenge in both approaches.

3.1.4 Conclusion of Preliminary Work

After a series of unsuccessful attempts, we concluded that alternative strategies were needed. The goal shifted toward identifying a new method for influencing the formation of origami patterns in thin shells—one that could serve as a foundational tool for a wide range of applications. This project is not tied to a specific application but rather aims to establish fundamental principles for deployable origami-based structures across various fields.

3.2 Design of Origami Patterns Using Parametric Code

To enable rapid design iterations and test multiple configurations, origami structures were generated programmatically using Python and Matplotlib. In this setup, vertices are defined as 3D points and connected to form facets.

We focused on Yoshimura and Kresling patterns due to their relevance in buckling and torsional response of cylindrical shells. Both were implemented via geometric algorithms.

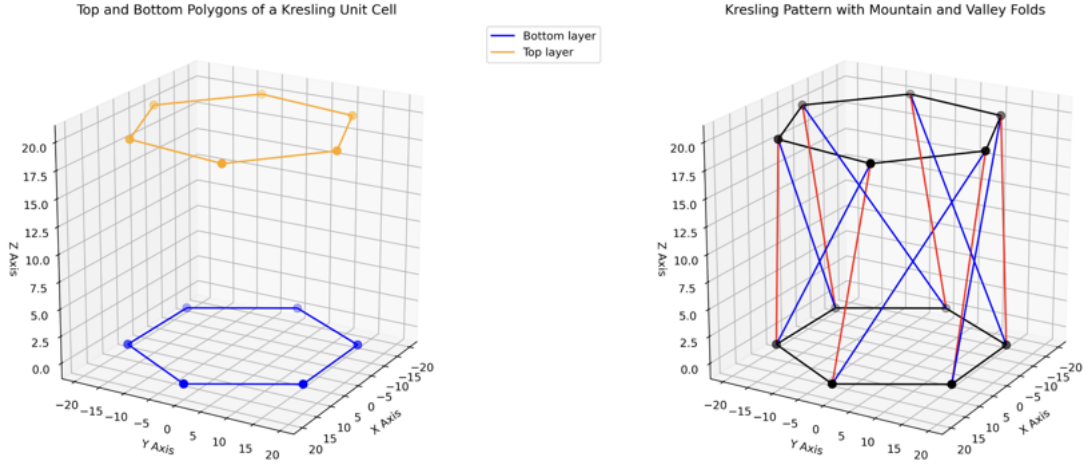


Figure 20: Wireframe of a Kresling unit cylindrical layer

The Kresling pattern is constructed by generating two sets of points arranged in circles: one on the bottom layer and one on the top. The angular spacing between points is uniform and determined by the number of facets. To introduce the characteristic twist of the Kresling structure, a constant angular offset is applied to the top layer. The polygonal panels of the structure are defined by connecting these points with edges. Each edge represents a fold and is classified as either a mountain fold or a valley fold. Valley folds bend inward toward the cylinder axis, while mountain folds bend outward, creating the distinct origami-like deformation behavior.

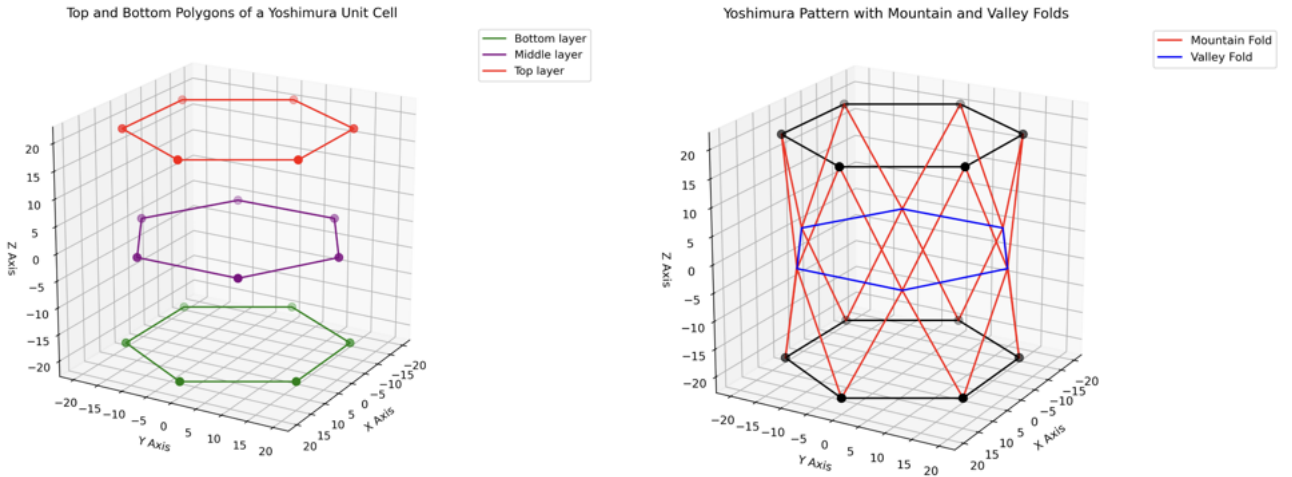


Figure 21: Wireframe of a Yoshimura unit cylindrical layer

The Yoshimura pattern is generated by placing three stacked layers of polygonal points: bottom,

middle, and top. Each layer consists of points evenly distributed around a circle, with the middle layer angularly offset by half the angle between vertices. This offset creates the characteristic diamond geometry of the Yoshimura pattern.

Edges connecting these points represent fold lines. Radial connections between the middle layer and the top or bottom layers are labeled as mountain folds, which bend outward from the surface. Diagonal connections form valley folds, which bend inward. The arrangement of these folds creates the repeating diamond-shaped facets observed in post-buckled cylindrical shells with axial compression.

While Python was used for initial prototyping, CAD tools were needed for exportable geometry (e.g., STL, STEP). Fusion 360 was chosen for its Python API, allowing automation of sketching and modeling operations. This scripting approach mirrors the GUI's feature-tree logic and allows manual adjustments post-automation, providing flexibility for users without programming experience.

3.2.1 Parametric CAD Code with Fusion 360

Fusion 360 provides the capability to design CAD parts and assemblies through scripting, which opens significant opportunities for automation and integration of AI-driven design tools. Among modern AI methods, Large Language Models (LLMs) are particularly powerful. As their name suggests, LLMs excel at processing and generating language. Consequently, describing mechanical parts through scripts creates a natural bridge between physical objects and language, enabling the possibility of generating or modifying CAD parts directly via natural language prompts.

Before exploring the potential of AI-assisted design, it is essential to understand the workflow of creating CAD parts through scripting. Fusion 360 is an attractive platform for this purpose: it is free for students, provides robust documentation, and offers an accessible Python API for parametric design.

The workflow typically begins by selecting a construction plane on which a sketch is created. Within a sketch, the user can manually draw or program the creation of geometric elements such as circles, rectangles, lines, polygons, and points. Constraints and dimensions can then be applied to define the sketch parametrically. If the sketch is defined correctly, Fusion 360's CAD engine automatically detects closed loops, which can be converted into 3D features via operations like extrusions and revolutions.

Once 3D bodies are generated, additional operations become available, such as mirroring and patterning. These features reduce redundant sketches by reusing geometry. For example, an origami pattern typically consists of a small unit cell repeated around a cylinder. Instead of creating each instance individually, a single unit cell can be patterned, significantly simplifying the workflow.

Fusion 360 employs a Boundary Representation (BRep) model in which each edge, face, and vertex is labeled. These geometric elements can be used as references to define additional construction planes or guide the creation of subsequent sketches. This parametric and hierarchical workflow facilitates efficient and automated design, forming a solid foundation for future AI-driven CAD generation.

3.2.2 Yoshimura Pattern

A base polygon (6 sides, 40 mm radius) is sketched on the XY plane and fully constrained using a vertical construction line. A second sketch plane is offset 15 mm along Z, where an identical polygon is drawn. An angle constraint of $360^\circ/(2 \times \text{sides})$ is added between the vertical reference and a line to the first vertex, defining the Yoshimura diamond shape.

Two planes are created using:

- Two vertices from the base polygon and one from the top.
- Two vertices from the top and one from the base.

Four construction points are added for reference.

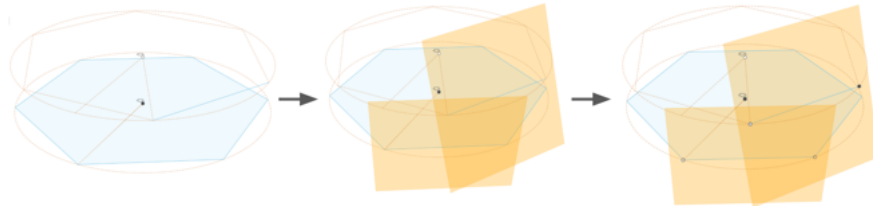


Figure 22: Offset polygons and construction planes created from vertex triplets. Reference points aid facet creation.

Triangles are sketched on the facet planes, constrained using projected lines. These are used to create surface patches. A circular pattern replicates the patches around the central axis.

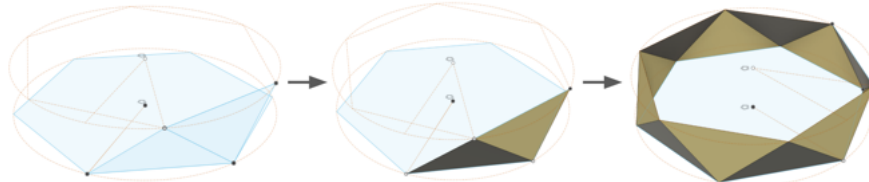


Figure 23: Facet patches sketched and repeated using circular pattern to complete a half Yoshimura layer.

The half-layer is mirrored across the offset plane to complete a full layer. Repetition along Z forms a cylinder of desired length.

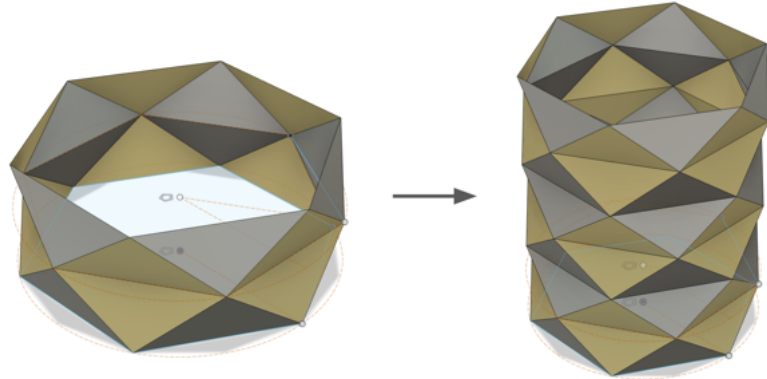


Figure 24: Full Yoshimura layer obtained by mirroring and repeating along the Z-axis.

For testing (e.g., compression), connector surfaces are added. Circular profiles are lofted from the base polygon, then all surfaces are stitched. A thickness of 2 mm is applied to convert the surface into a solid body.

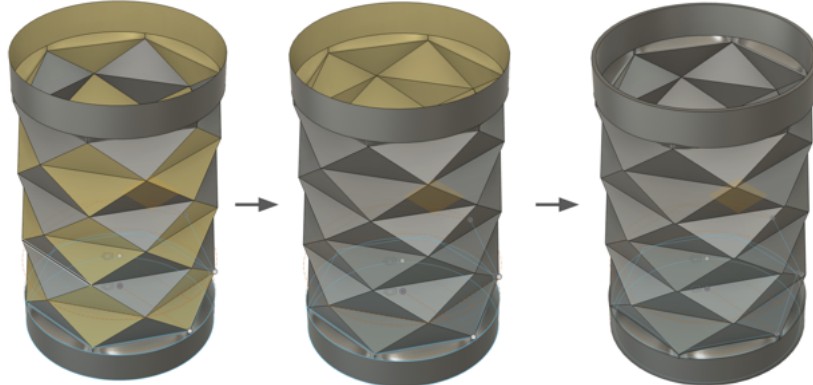


Figure 25: Connector lofts and patch stitching. Final body thickened to 2mm.

3.2.3 Kresling Pattern

The Kresling pattern was modeled similarly, with parametric control over height, radius, and twist angle. A triangular unit cell was constructed and patterned in rotation and height.

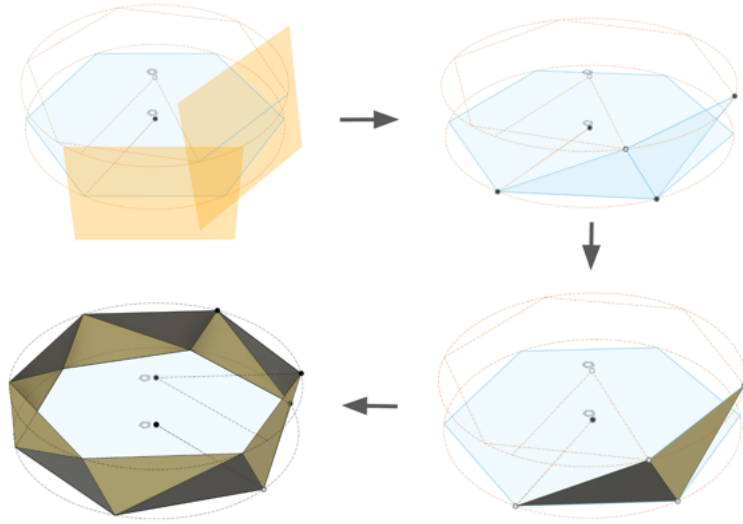


Figure 26: Kresling CAD construction showing unit facets and geometric assembly.

Different twist angles were tested to study the effect on mechanical behavior and deformation modes.



Figure 27: Effect of twist angle on Kresling unit geometry.

3.3 Computational methods

3.3.1 Simulation of the Complete Mechanism

Two types of finite element simulations were considered to model the mechanical behavior of the origami metamaterial:

- **Shell Elements:** Suitable for thin structures where bending dominates. Shell meshes can be constructed using either triangular or quadrilateral elements. In CalculiX, triangular shell elements are labeled as S6 (6-node elements), while quadrilateral elements are labeled as S8R (8-node elements with reduced integration). The shell element simulation is more computationally efficient than a solid simulation model and can be adequate for thin origami structures similar to paper structures.
- **Solid Elements:** More appropriate for thick or volumetric structures where through-thickness stress distribution matters. CalculiX provides the C3D10 element—a 10-node tetrahedral element—for simulating such 3D solid geometries. The solid element modeling is suited for origami material where the thickness variation contributes to the crease and pannel design. By that I am mostly thinking about the living hinge origami materials.

Why CalculiX? One of the main advantages of using CalculiX is that it is open-source and free, making it accessible to a broader research community—particularly those who may not have access to commercial tools like Abaqus. This democratization of finite element simulation fosters innovation in the study and design of origami-based metamaterials.

Automation and Usability. Despite its capabilities, setting up simulations in CalculiX can be complex and time-consuming. To address this, we developed a Python-based interface that automates the process of geometry definition, mesh generation, boundary condition specification, and job submission. This tool significantly lowers the barrier to entry and streamlines the simulation workflow.

Element Selection Considerations. A crucial question in any FEA study is: **What is the most suitable element type for my structure?** The answer depends on several factors, including geometric complexity, thickness-to-span ratio, deformation modes, and computational cost. For origami-inspired structures, which are often thin and exhibit significant bending and folding, shell elements generally provide a good balance between accuracy and efficiency.

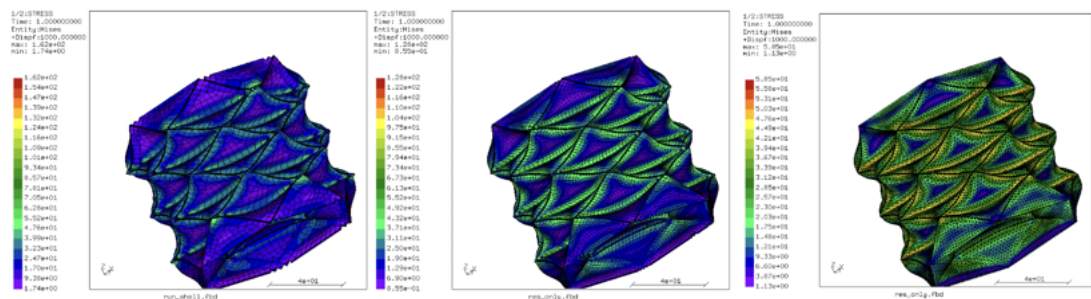


Figure 28: Shell-based simulations of the structure. The first two cases use quadrilateral shell elements with different mesh densities, while the third case uses triangular shell elements.

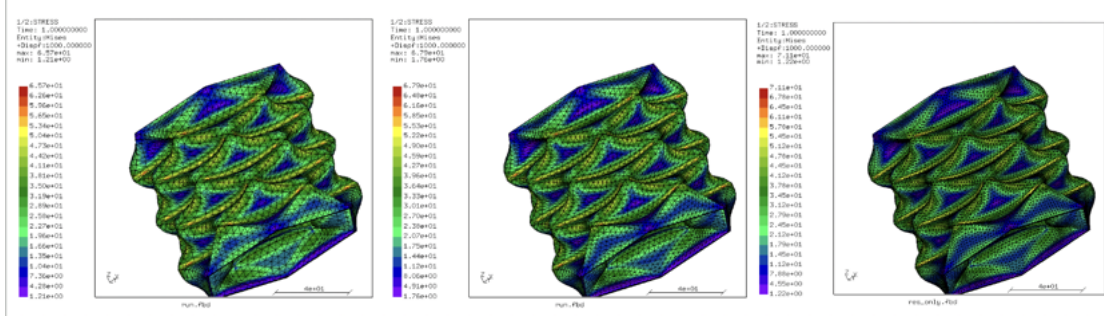


Figure 29: Simulation results obtained using solid C3D10 elements.

3.3.2 Design and simulation of living hinges

To create a functional crease without relying on a secondary elastomeric material to connect two rigid panels, we must develop a design strategy that enables the programming of a preferred folding direction between rigid sections. Such “living hinges” are widely used in the injection molding industry, for example, in the fabrication of integral lid hinges. One common approach involves introducing localized regions of reduced thickness to concentrate deformation along the desired fold lines.

In our case, the objective is to design crease lines with an intrinsic bias for folding in a predetermined direction under load, thereby guiding the overall deformation toward the emergence of targeted origami patterns. At the same time, the integrity of the entire structure must be preserved. As a result, we cannot rely solely on reducing the thickness of the material at the hinge, especially given the mechanical properties and resolution constraints of our chosen fabrication method—SLA 3D printing. We therefore explore alternative strategies for creating effective living hinges that retain the full thickness of the adjacent panels, enabling precise control over folding behavior without compromising structural strength.

To gain insight into how two panels connected by a crease deform under load, and to evaluate the resulting stress distribution, we rely on Finite Element Analysis (FEA). For this purpose, we use **CalculiX**, an open-source FEA software that offers reliable results comparable to commercial tools such as Abaqus. Although CalculiX provides limited graphical user interface capabilities, it remains a practical tool for setting up and running simulations, especially when combined with custom preprocessing scripts. In our workflow, geometries are first prepared in CAD and meshed using **Gmsh**, with simulation setups scripted and exported as **.inp** files. These are then processed by CalculiX, allowing for flexible automation and customization of the simulation pipeline.

To isolate and study the effect of the living hinge or crease geometry, all simulations are performed using a standardized sample. Each model consists of two rigid panels forming a single block with fixed dimensions: 30 mm in width, 80 mm in length, and 10 mm in thickness. This consistency across simulations allows us to focus solely on how variations in the crease design influence the mechanical response.

The first step in the finite element analysis is meshing, which is a critical factor in the accuracy and stability of the simulation. We use **C3D10** elements—10-node quadratic tetrahedral elements—due to their versatility and reliability for 3D solid mechanics problems. A maximum element size of 2 mm is selected to balance accuracy with computational efficiency, considering

the constraints of the available hardware (a MacBook Air with an M2 chip).

The nodes of the mesh fall into three categories:

1. **Internal nodes**, which form the body of the mesh.
2. **Support (clamped) nodes**, located on one end face of the first panel, where all degrees of freedom are constrained to simulate a fixed boundary condition.
3. **Prescribed displacement nodes**, situated on the opposite end face of the second panel, where a displacement vector is applied to simulate compressive loading.

This loading setup induces folding across the central crease, enabling the evaluation of how different crease geometries influence stress distribution and deformation under compression.

To illustrate the simulation setup and the implemented living hinge geometry, Figure 37 shows a representative 3D plot of one of the analyzed samples.

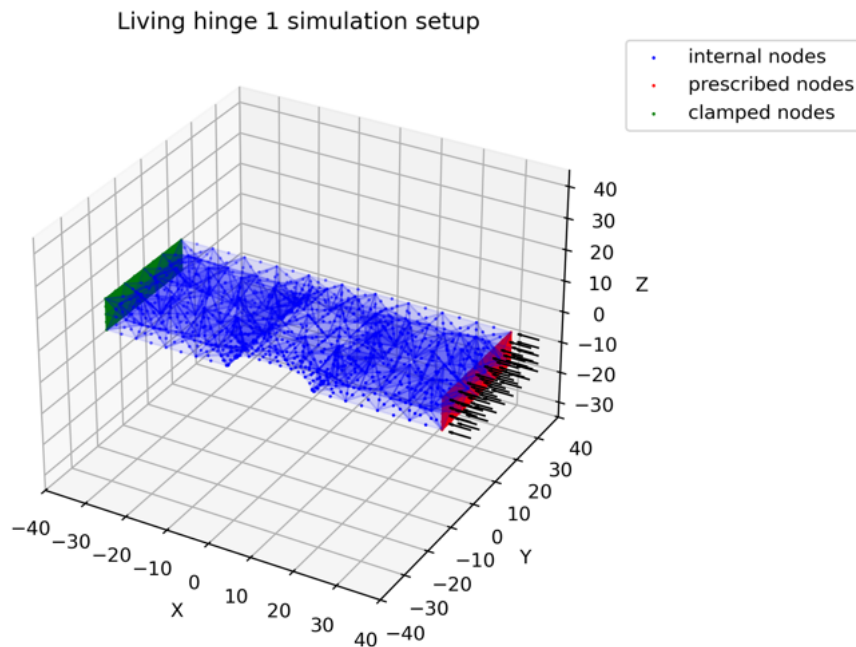


Figure 30: 3D visualization of the finite element mesh for a sample with a living hinge created by a surface sweep cut. Node types are color-coded: internal (blue), clamped (green), and prescribed displacement (red).

In this example, the living hinge is created by sweeping a cut that removes a thin layer of material from one face of the block. The concept behind this design is to locally reduce stiffness, thereby encouraging the panels to fold preferentially along the weakened line under compression. In the 3D plot, the mesh structure is fully visible, with element faces represented as interconnected nodes and edges. The visualization highlights different types of nodes according to their function:

- **Blue** indicates internal nodes, which make up the bulk of the mesh.

- **Green** corresponds to support nodes located on the clamped face of the panel.
- **Red** marks the nodes on the displacement face, where a compressive displacement vector is applied.

CalculiX operates in a workflow similar to that of Abaqus. The main driver of the simulation is an input file (.inp), which references geometry and mesh data defined in external files. In our setup, the mesh—including node and element definitions—is stored in all.msh, while node sets for boundary conditions are provided in support.nam (for the clamped face) and displacement.nam (for the loading face). The .inp file specifies the material properties, element type, boundary conditions, and the displacement vector applied to simulate compression.

The simulation is executed by running the command ccx living_hinge.inp in the terminal. This launches CalculiX, which processes the input and generates a series of result files. The most critical output is the .frd file (living_hinge.frd), which contains nodal displacement data, stress fields, and other simulation results.

To visualize these results, the .frd file is post-processed using CGX (CalculiX GraphiX), the graphical interface of CalculiX. By issuing a sequence of CGX commands, we can render the deformed shape of the structure with color maps representing the von Mises stress distribution. The color scale typically ranges from blue (low stress) through green (moderate stress) to red (high stress), offering a clear visual indication of how the structure responds to loading.

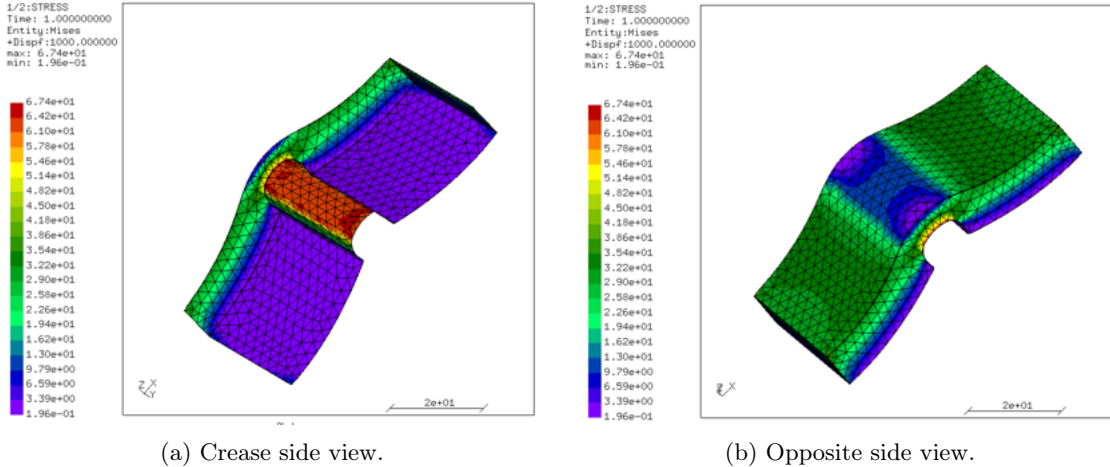


Figure 31: Deformed shape of the sample under compression, viewed from both the crease side and the opposite side. Node types are color-coded: internal (blue), clamped (green), and prescribed displacement (red).

These post-processing visualizations clearly reveal a preferred direction of deformation centered around the sweep line where material was removed. The stress distribution shows high concentration on the inner side of the crease, where compression is most severe, and minimal stress on the outer side, validating the effectiveness of the crease design in guiding the fold.

3.4 Semi-analytical Method

This method describes the simulation framework for origami structures using a bar-and-hinge model. We focus specifically on metamaterials composed of triangular patterns, such as Kresling and Yoshimura cylinders. In these cases, the mechanical behavior can be accurately captured by modeling panel stretching using bar elements and folding along crease lines using rotational springs.

If the panels were quadrilateral (e.g., rectangular), modeling would additionally require incorporating bending behavior across panel surfaces, typically represented by diagonal fold lines. However, since we restrict our analysis to triangular panels, we neglect panel bending and focus solely on axial deformation (bars) and hinge rotation (springs).

At each step of the simulation, the total potential energy of the system is computed as the sum of internal strain energy (stored in bars and rotational springs) and external work due to applied loads. The potential energy depends only on the current configuration, independent of deformation history, assuming purely elastic behavior.

$$\Pi = U_{\text{bar}} + U_{\text{spr}} - V_{\text{ext}} \quad (1)$$

The equilibrium configuration corresponds to a stationary point of the potential energy. This is achieved when its first variation vanishes:

$$D\Pi \delta \mathbf{v} = \delta \mathbf{v}^\top \mathbf{R} = 0 \quad (2)$$

Here, $\mathbf{R}(\mathbf{u})$ is the residual force vector, defined as:

$$\mathbf{R}(\mathbf{u}) = \mathbf{T}_{\text{bar}}(\mathbf{u}) + \mathbf{T}_{\text{spr}}(\mathbf{u}) - \mathbf{F}(\mathbf{u}) = 0 \quad (3)$$

To solve this nonlinear equilibrium equation, we linearize it around the current configuration. This leads to the tangent stiffness formulation:

$$D\mathbf{R} \delta \mathbf{u} = \mathbf{K} \delta \mathbf{u} \quad (4)$$

The global stiffness matrix \mathbf{K} is decomposed into the contributions from the bars and rotational springs:

$$\mathbf{K}(\mathbf{u}) = \mathbf{K}_{\text{bar}}(\mathbf{u}) + \mathbf{K}_{\text{spr}}(\mathbf{u}) \quad (5)$$

3.4.1 Finite Element Formulation of Bar Elements

We adopt a hyperelastic formulation for the bar elements, which provides greater generality and accuracy than linear elasticity—especially for materials undergoing large deformations. The strain energy density function W , defined in terms of the Green-Lagrange strain E_X , is used to model the internal energy stored in each bar element. The cross-sectional area $A^{(e)}$ of each element is assumed constant along its length.

The total stored energy in a bar element e is expressed as:

$$U_{\text{bar}}^{(e)} = \int_0^{L^{(e)}} W A^{(e)} dX \quad (6)$$

Assuming linear shape functions, the one-dimensional Green-Lagrange strain E_X is given by:

$$E_X = \mathbf{B}_1 \mathbf{u}^{(e)} + \frac{1}{2} (\mathbf{u}^{(e)})^\top \mathbf{B}_2 \mathbf{u}^{(e)} \quad (7)$$

where $\mathbf{u}^{(e)}$ is the displacement vector of the two bar nodes:

$$\mathbf{u}^{(e)} = [u_a, v_a, w_a, u_b, v_b, w_b]^\top \quad (8)$$

The matrices \mathbf{B}_1 and \mathbf{B}_2 are defined as:

$$\mathbf{B}_1 = \frac{1}{L^{(e)}} [-\mathbf{e}_1 \quad \mathbf{e}_1], \quad \mathbf{B}_2 = \frac{1}{(L^{(e)})^2} \begin{bmatrix} \mathbf{I}_{3 \times 3} & -\mathbf{I}_{3 \times 3} \\ -\mathbf{I}_{3 \times 3} & \mathbf{I}_{3 \times 3} \end{bmatrix} \quad (9)$$

The internal force vector for bar element e is obtained as:

$$\mathbf{T}_{\text{bar}}^{(e)} = S_X A^{(e)} L^{(e)} (\mathbf{B}_1^\top + \mathbf{B}_2 \mathbf{u}^{(e)}) \quad (10)$$

where S_X is the second Piola-Kirchhoff stress component. Linearizing this force with respect to displacements yields the tangent stiffness matrix:

$$\mathbf{K}_{\text{bar}}^{(e)} = C A^{(e)} L^{(e)} (\mathbf{B}_1^\top + \mathbf{B}_2 \mathbf{u}^{(e)}) (\mathbf{B}_1^\top + \mathbf{B}_2 \mathbf{u}^{(e)})^\top + S_X A^{(e)} L^{(e)} \mathbf{B}_2 \quad (11)$$

Here, C is the tangent modulus, defined as:

$$C = \frac{\partial S_X}{\partial E_X} \quad (12)$$

3.4.2 Symmetric Tangent Stiffness Matrix Expansion

The tangent stiffness matrix can be decomposed into physically meaningful components:

$$\mathbf{K}_{\text{bar}}^{(e)} = \mathbf{K}_E^{(e)} + \mathbf{K}_1^{(e)} + \mathbf{K}_2^{(e)} + \mathbf{K}_G^{(e)} \quad (13)$$

where:

$$\mathbf{K}_E^{(e)} = C A^{(e)} L^{(e)} \mathbf{B}_1^\top \mathbf{B}_1 \quad (14)$$

$$\mathbf{K}_1^{(e)} = C A^{(e)} L^{(e)} ((\mathbf{B}_2 \mathbf{u}^{(e)}) \mathbf{B}_1 + \mathbf{B}_1^\top (\mathbf{B}_2 \mathbf{u}^{(e)})^\top) \quad (15)$$

$$\mathbf{K}_2^{(e)} = C A^{(e)} L^{(e)} (\mathbf{B}_2 \mathbf{u}^{(e)}) (\mathbf{B}_2 \mathbf{u}^{(e)})^\top \quad (16)$$

$$\mathbf{K}_G^{(e)} = S_X A^{(e)} L^{(e)} \mathbf{B}_2 \quad (17)$$

To express \mathbf{B}_1 in global coordinates, we use the directional cosines of the bar:

$$\tilde{\mathbf{B}}_1 = \frac{1}{L^{(e)}} \left[-\left(\frac{\mathbf{X}_b - \mathbf{X}_a}{L^{(e)}} \right)^\top \quad \left(\frac{\mathbf{X}_b - \mathbf{X}_a}{L^{(e)}} \right)^\top \right] \quad (18)$$

where \mathbf{X}_a and \mathbf{X}_b are the initial global coordinates of the bar's end nodes.

3.4.3 Rotational Spring Elements

Rotational spring elements are used to model fold lines or bending diagonals between two adjacent triangular panels. Each such element consists of four nodes defining two triangles that lie on intersecting planes. The relative rotation between the triangles is measured by the dihedral angle θ , which fully determines the configuration of the fold.

We assume that the stored energy in each rotational spring is a function $\psi(\theta)$ of the dihedral angle:

$$U_{\text{spr}}^{(r)} = \psi(\theta) \quad (19)$$

The resistance moment M associated with the rotational spring is obtained as the derivative of the energy with respect to θ :

$$M = \frac{\partial \psi(\theta)}{\partial \theta} \quad (20)$$

The internal force vector is then given by the chain rule as:

$$\mathbf{T}_{\text{spr}}^{(r)}(\mathbf{u}) = \tilde{\mathbf{T}}_{\text{spr}}^{(r)}(\mathbf{x}) = M \frac{d\theta}{d\mathbf{x}^{(r)}} \quad (21)$$

Since we directly work in global coordinates and $\mathbf{u} = \mathbf{x} - \mathbf{X}$, no coordinate transformation is required. Differentiating the internal force vector with respect to displacements gives the tangent stiffness matrix:

$$\mathbf{K}_{\text{spr}}^{(r)}(\mathbf{u}) = \tilde{\mathbf{K}}_{\text{spr}}^{(r)}(\mathbf{x}) = k \frac{d\theta}{d\mathbf{x}^{(r)}} \otimes \frac{d\theta}{d\mathbf{x}^{(r)}} + M \frac{d^2\theta}{d(\mathbf{x}^{(r)})^2} \quad (22)$$

Here, \otimes denotes the tensor (outer) product, and k is the tangent rotational stiffness defined as:

$$k = \frac{dM}{d\theta} \quad (23)$$

This formulation generalizes the rotational spring model beyond the linear case, allowing for non-linear constitutive behaviors depending on the dihedral angle. We assume no coupling between the in-plane behavior (modeled by bars) and the out-of-plane rotational springs.

3.4.4 Dihedral Angle and Vector Definitions

To robustly compute the dihedral angle between two origami panels without encountering singularities, we represent a fold as the intersection of two planes. This intersection defines the *crease line*. In both trihedral and quadrilateral origami structures (e.g., Miura-ori), a fold can be described by four nodes forming two triangles. For instance, the node sets $\{i, j, k\}$ and $\{j, k, \ell\}$ define two triangles lying in distinct planes, intersecting along the shared edge $j \rightarrow k$.

Let $\mathbf{x}_p^{(r)}$ denote the position of node p in the current configuration. We define the edge vector between any two nodes p and q as:

$$\mathbf{r}_{pq} = \mathbf{x}_p^{(r)} - \mathbf{x}_q^{(r)} \quad (24)$$

Using this, we compute the normal vectors to the two triangles:

$$\mathbf{m} = \mathbf{r}_{ij} \times \mathbf{r}_{kj}, \quad \mathbf{n} = \mathbf{r}_{kj} \times \mathbf{r}_{k\ell} \quad (25)$$

The unsigned dihedral angle θ between the two planes is then defined by:

$$\theta = \arccos \left(\frac{\mathbf{m} \cdot \mathbf{n}}{\|\mathbf{m}\| \|\mathbf{n}\|} \right) \quad (26)$$

However, this definition only captures angles in the range $[0, \pi]$ and does not distinguish between mountain and valley folds. To ensure a smooth and continuous description over the full range $[0, 2\pi)$, we define the signed dihedral angle as:

$$\theta = \eta \arccos \left(\frac{\mathbf{m} \cdot \mathbf{n}}{\|\mathbf{m}\| \|\mathbf{n}\|} \right) \mod 2\pi \quad (27)$$

where the sign indicator η is given by:

$$\eta = \begin{cases} \text{sgn}(\mathbf{m} \cdot \mathbf{r}_{k\ell}), & \mathbf{m} \cdot \mathbf{r}_{k\ell} \neq 0 \\ 1, & \mathbf{m} \cdot \mathbf{r}_{k\ell} = 0 \end{cases} \quad (28)$$

This formulation allows for continuous tracking of the fold angle from 0 to 2π , thereby naturally accommodating the transition between mountain and valley folds. The flat state corresponds to $\theta = \pi$, which is treated as a regular configuration within this energy-based framework.

3.4.5 Simulation Testing of Origami Materials

To evaluate the mechanical response of origami structures, two classical types of tests were implemented in our simulation: load-controlled and displacement-controlled experiments.

- **Load-Controlled Compression Test:** In this test, the nodes lying on the bottom plane are fixed in all directions, constraining their displacement. A compressive load is then applied in the Z-direction on the top nodes. The simulation computes the displacement vector of the free nodes over a predefined number of iterations using a nonlinear solver to capture the deformation response of the structure.

- **Displacement-Controlled Compression Test:** In the second experiment, a displacement is prescribed incrementally on the top nodes in the Z-direction, while the bottom nodes remain fixed. At each step, the internal forces and resulting reaction loads are computed based on the current configuration. Unlike the load-controlled case, this approach does not require solving an energy minimization problem via the Newton-Raphson method. Instead, the global stiffness matrix is updated at each step to directly evaluate the structural response.

In both method we output the displacement of each free Nodes. The force in those bars as well as the momentum between each panels on each crease lines is recorded at each increments.

3.5 3D Printing of Origami Metamaterials

To fabricate the origami-inspired metamaterials, we employed a high-resolution LCD-based stereolithography (SLA) 3D printer. This additive manufacturing method is based on masked photopolymerization, a subset of vat photopolymerization in which a UV-backlit LCD screen selectively cures photosensitive resin layer-by-layer.

Manufacturing Process

In SLA printing, the build platform lowers into a vat filled with UV-curable resin. The vat base incorporates a flexible, transparent film—typically fluorinated ethylene propylene (FEP) or its non-fluorinated variant (NFEP)—which provides optical clarity and easy part release. A collimated 405 nm LED light source, spatially modulated by an LCD mask, selectively polymerizes the resin at each layer. The platform then incrementally lifts to allow resin replenishment before curing the next layer. This bottom-up approach enables the fabrication of highly detailed structures with complex internal features, which would be difficult to manufacture using conventional methods.

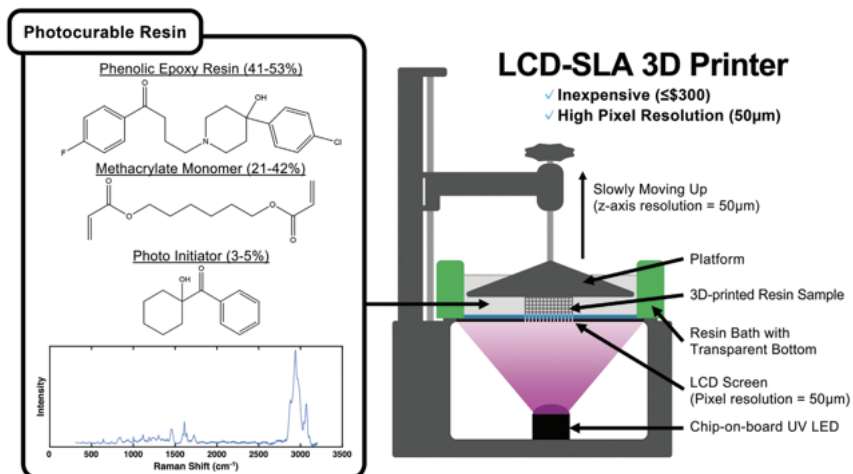


Figure 32: Schematic of the LCD-based vat photopolymerization process used to fabricate flexible origami metamaterials, highlighting the layer-by-layer curing mechanism.

Design and Processing Workflow

Origami geometries were generated using parametric scripts that allow systematic variation of fold patterns, panel dimensions, and hinge geometries. The models were exported as stereolithography (STL) files from Fusion 360 and sliced using ChiTuBox software, which prepares the print by discretizing the geometry into 2D cross-sections and assigning exposure settings for each layer.

Material Selection and Processing Parameters

To meet the requirements for flexibility and large reversible deformation, a specialized elastomeric resin was selected. Such resins typically have lower photoreactivity than rigid alternatives, requiring careful tuning of exposure parameters to ensure full crosslinking without sacrificing dimensional accuracy.

The process parameters were optimized as follows: initial adhesion layers were exposed for 30 seconds to ensure strong platform bonding, while subsequent layers received 6–8 seconds of UV exposure. These settings were calibrated based on manufacturer recommendations and empirical tests to balance curing completeness with fine-feature resolution.

Process-Related Defects and Mitigation Strategies

Exposure calibration is crucial to prevent common printing defects:

- **Underexposure:** Insufficient UV energy can result in incomplete polymerization, leading to delamination, warping, and mechanical failure at overhangs or thin features.
- **Overexposure:** Excessive UV light causes feature distortion due to lateral light bleeding (the blooming effect), loss of dimensional fidelity, and smearing of critical hinge geometries.

Post-Processing Protocol

A standardized post-processing sequence was applied to ensure optimal mechanical performance:

1. **Initial cleaning:** Parts were carefully removed from the build platform and immersed in isopropyl alcohol (IPA) under ultrasonic agitation for 10 minutes to remove uncured resin.
2. **Secondary rinse:** Components were gently rinsed in fresh IPA to eliminate redeposited contaminants.
3. **UV post-curing:** Samples were exposed to 405 nm UV light for 15 minutes to complete the crosslinking process. This step is critical for elastomeric resins, where post-curing significantly influences mechanical strength, elongation, and fatigue resistance.

Surface tackiness caused by oxygen inhibition during curing was mitigated via controlled ambient exposure; however, no inert atmosphere (e.g., nitrogen chamber) was used in the current setup.

This comprehensive workflow enabled the production of mechanically robust, foldable metamaterials suitable for experimental validation and integration into soft mechanical systems.

4 Results and Discussion

4.1 Full Pipeline

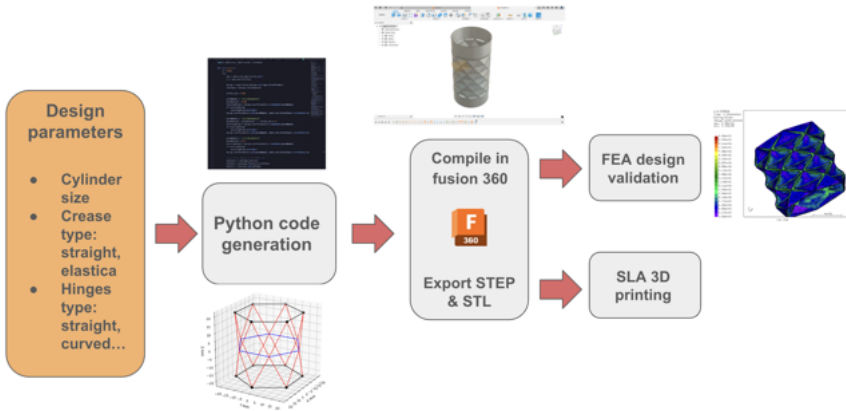


Figure 33: Overview of the ORIGAMI-STUDIO workflow, from parametric design to simulation and manufacturing.

This project led to the creation of an open-source software package called **ORIGAMI-STUDIO**. The software streamlines the entire workflow for designing, simulating, and manufacturing origami tubular structures. Two simulation approaches are integrated: a full Finite Element Analysis (FEA) method for high-fidelity mechanical evaluation, and a semi-analytical approach that allows faster parametric studies. The full code is publicly available at: <https://github.com/hugo-peni/ORIGAMI-STUDIO>.

The workflow begins with the user defining the key parameters of the structure: the target cylinder dimensions, the type of origami pattern, and the crease design. In this work, we focused on Kresling and Yoshimura patterns, which are well-suited for cylindrical structures undergoing compression and torsion. Creases can be either straight, as in traditional paper folding, or curved, which allows for smoother and more controlled deformation. Users may also integrate engineered features such as living hinges to further guide the folding process. Once the parameters are set, a wireframe of the origami cylinder is automatically generated in Python, providing a quick visual verification before proceeding to CAD creation.

The next stage is the parametric CAD generation. ORIGAMI-STUDIO automatically produces a Python script that leverages the Fusion 360 API to replicate CAD operations programmatically. Internally, the system relies on template scripts for each supported pattern (Kresling, Yoshimura, and curved-crease variants), which are modified according to the chosen parameters. When executed in Fusion 360, this script creates a fully parametric model of the origami structure and saves both STEP and STL files. The STEP file is used for meshing and simulation, while the STL file is directly suitable for additive manufacturing. Although the process is automated, the user can still access the CAD feature tree to make manual adjustments or refinements as needed. This approach significantly accelerates the exploration of multiple design variations while avoiding repetitive CAD tasks.

Before moving to manufacturing, the structure can be validated through automated FEA simulations. The default scenario applies a prescribed compression up to 90% of the initial cylinder height, allowing the user to observe the folding sequence and identify stress concentrations. The design philosophy focuses on concentrating deformation along the creases while keeping the panels as rigid as possible, leading to predictable and repeatable folding mechanics. These simulations provide valuable insight into the mechanical behavior of the structure and help avoid trial-and-error in the laboratory.

Once the design is validated, the STL file can be processed in Chitubox and printed using the lab's SLA 3D printers. This workflow enables rapid prototyping of origami metamaterials at different scales, while ensuring that each design has been pre-validated through simulation. Overall, ORIGAMI-STUDIO establishes a seamless pipeline that links parametric design, automated simulation, and manufacturing, significantly accelerating the study and application of origami-based structures.

4.2 Playing with Multiple Designs

To explore the design space of origami metamaterials, multiple pattern variations were generated and tested using **ORIGAMI-STUDIO**. The simplest configurations are the classical Yoshimura and Kresling patterns with straight creases, as shown in Figure 34. These provide a baseline for cylindrical structures capable of folding under axial compression, with Kresling patterns also allowing torsional motion.

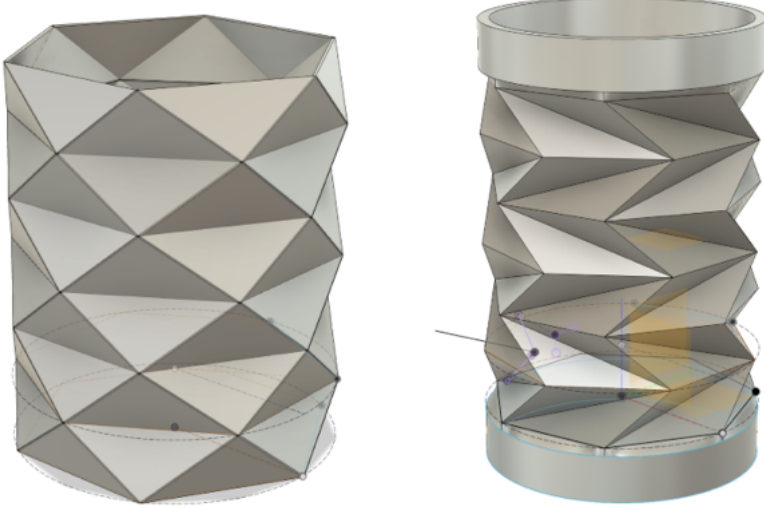


Figure 34: Examples of baseline origami geometries: (left) Kresling pattern, (right) Yoshimura pattern with straight creases.

Beyond straight creases, the same origami pattern can be radically transformed by adopting **curved creases** that follow an *elastica* profile, as shown in Figure 35. Compared to sharp straight creases, elastica-based folds introduce a continuous curvature, which provides several mechanical benefits:

- They **smooth stress concentrations**, reducing the likelihood of panel cracking or undesired local buckling.
- They **promote a more gradual and controlled folding sequence**, improving repeatability.
- They **enhance energy absorption** by allowing panels to bend progressively along the curve, instead of concentrating deformation at a single sharp fold.

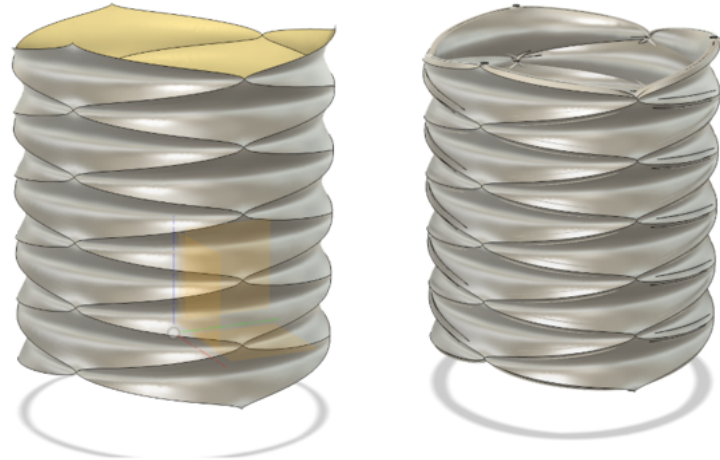


Figure 35: Curved-crease Yoshimura origami pattern. Elastica folds provide smoother deformation and enhanced mechanical control.

Another critical design aspect involves the **panel interface**, which determines how the panels are allowed to deform. Figure 36 compares two Yoshimura configurations with embedded living hinges:

- Left: A single-layer cylinder with hinges following a curved path.
- Right: A slit-based hinge pattern, allowing panels to flex along predefined lines.

FEA simulations and experimental observations indicate that living hinges **enhance the predictability of folding** by localizing deformation where intended. They transform the origami into a mechanically guided system, where the folding kinematics are repeatable and less prone to uncontrolled global buckling.



Figure 36: Exploring panel interfaces with living hinges: (left) curved hinge pattern, (right) slit-based hinge pattern.

This systematic exploration of different crease geometries and panel interfaces forms the foundation for defining design guidelines that balance **manufacturability**, **mechanical efficiency**, and **folding predictability**. These variations—straight vs. curved creases and rigid vs. compliant interfaces—represent key design levers for tailoring the mechanical response of origami metamaterials.

4.3 The Choice of the Panel Interface

One of the key contributions of this thesis is the exploration of different crease geometries, ranging from simple sharp pre-creases to compliant living hinges. This design choice profoundly influences the mechanical response of origami metamaterials, affecting stress distribution, deformation localization, and overall kinematic predictability.

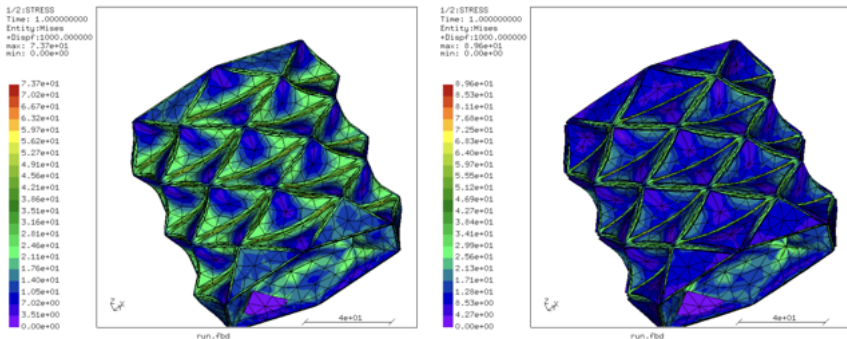


Figure 37: Compression test comparison of two Yoshimura origami structures: (left) with sharp pre-creases only, and (right) with embedded living hinges at fold lines.

Finite Element Analysis (FEA) and compression tests reveal a stark contrast between the two approaches. Structures with living hinges exhibit well-localized deformation along the intended fold lines. The compliant hinge zones act as mechanical filters, channeling stresses into the creases and preserving the rigidity of the surrounding panels. By contrast, sharp pre-creases tend to produce more diffuse deformation, where bending spreads into the panels, reducing structural efficiency and predictability.

Living hinges provide several mechanical advantages. First, they maintain panel rigidity by confining flexibility to narrow hinge zones.

This promotes well-defined and repeatable folding kinematics, while also minimizing the risk of global buckling. Additionally, load paths are more controlled, as stresses are concentrated along predefined flexural regions, improving energy absorption and reliability in load-bearing scenarios.

The pre-crease approach remains simpler to manufacture in certain contexts, especially when using paper, polymer sheets, or thin metal foils that can be folded directly. However, this simplicity comes at the cost of mechanical selectivity. In contrast, living hinges transform the origami into a more controlled mechanical system with predictable folding behavior. From a manufacturing perspective, the added complexity of living hinges is negligible in the context of SLA 3D printing, which can seamlessly integrate them into the printed geometry. However, industrial processes such as metal sheet bending or polymer thermoforming may face additional challenges in replicating hinge-like features.

These design considerations open the door to a wide range of origami metamaterial applications. Yoshimura patterns can serve as compactable energy-absorbing systems under axial compression, suitable for damping or impact mitigation. Kresling patterns, by contrast, offer an additional degree of freedom: they can deform under both compression and torsion. This makes them ideal for protective sleeves on robotic arms, where twisting and axial motion must coexist. Another promising application is the development of expandable, watertight containers that fold into compact volumes for storage and deploy on demand, a concept enabled by SLA 3D printing.

In summary, the choice of crease geometry—pre-crease or living hinge—acts as a fundamental design lever in origami metamaterials. Through FEA-driven analysis and prototyping, this thesis establishes design guidelines that link crease geometry to folding predictability, structural efficiency, and potential application domains.

4.4 Manufacturing

The final stage of the workflow is the physical realization of the origami structures through additive manufacturing. Once the STL file is exported from **ORIGAMI-STUDIO**, it can be directly processed in Chitubox and printed using the lab's SLA 3D printer (Elegoo Mars 5 Ultra). This printer leverages LCD-based stereolithography, enabling the fabrication of complex geometries with high resolution and smooth surfaces.

SLA printing offers several advantages for origami metamaterials:

- **High precision:** Fine crease features and thin living hinges can be produced without post-processing.

- **Speed:** Entire layers are cured simultaneously, making the process significantly faster than FDM printing.
- **Airtightness:** Resin prints are inherently non-porous, enabling watertight and air-sealed structures, which can be further improved by a final UV curing or resin coating.

Figure 38 shows an overview of the printing setup and a first Yoshimura cylinder fabricated in an elastomeric resin. Different scales and cell sizes were tested to assess the influence of geometry on foldability. Straight-crease cylinders could fold under compression, but their deformation was often unpredictable and prone to panel buckling. This limitation motivated the introduction of **living hinges**, which guided the deformation along predefined paths and significantly improved folding repeatability (Figure 40).



Figure 38: Left: SLA printer used for fabrication. Right: first 3D-printed Yoshimura cylinder in elastomeric resin.



Figure 39: Compression test of a Yoshimura cylinder with sharp pre-creases. Folding occurs but is not always controlled.

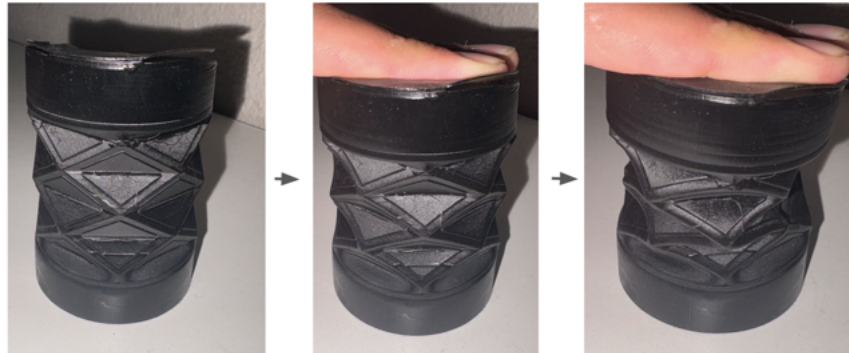


Figure 40: Compression test of a Yoshimura cylinder with living hinges. Deformation is localized and folding is highly predictable.

This stage validates the full digital-to-physical pipeline: parametric design → automated simulation → manufacturing-ready output. By integrating SLA 3D printing, the workflow supports rapid iteration and reliable production of origami metamaterials, bridging the gap between simulation and experimental validation.

4.5 Potential for Improvements

4.5.1 AI-Assisted Design Tools

Although the potential use of Large Language Models (LLMs) for generating parametric CAD scripts has been discussed, this aspect was not directly explored in the scope of this thesis. The

primary focus was to produce initial example scripts for origami metamaterials, which was a necessary foundation before meaningful AI-driven code generation could be pursued.

For LLMs to be effective in this context, they require structured data, contextual information, and representative examples of CAD scripting workflows. Currently, publicly available data on CAD script generation is extremely limited, and general-purpose LLMs perform poorly without such domain-specific resources. However, these models demonstrate significantly better performance when modifying or extending existing scripts rather than generating complete programs from scratch.

Future work could focus on curating a dedicated dataset of parametric CAD scripts and developing tailored AI workflows. Such tools could assist engineers in rapidly iterating, refining, and automating the design of parametric origami structures.

4.5.2 Expanding to Other Origami Patterns

Inspired by the work of Zhao’s lab on cylindrical spinner and crawling robots, our initial design efforts primarily focused on Kresling and Yoshimura patterns. These geometries are particularly well-suited for cylindrical structures undergoing twisting and compressive deformations. A key improvement to the software would be expanding its capabilities to include additional origami patterns, providing a broader design space and unlocking new functional properties.

For example, Waterbomb and Miura-ori patterns exhibit negative Poisson’s ratio (auxetic behavior), which makes them ideal for deployable and shock-absorbing structures. Eggbox and other multistable patterns could generate materials that lock into multiple configurations, highly valuable in robotics and aerospace. Incorporating curved-folding and hybrid patterns would further enhance flexibility, enabling smoother deformations and reducing stress concentrations.

Most current origami CAD tools are pattern-limited. The software we developed focuses primarily on cylindrical structures, while other available tools are often restricted to Miura-ori. Offering a hybrid, multi-pattern design software would provide a significant advantage. Such a tool would appeal both to researchers exploring new mechanical behaviors and to engineers seeking rapid prototyping of unusual folding geometries.

4.5.3 Enhancing the User Experience

Currently, we provide a collection of Python scripts to design and simulate origami metamaterials. While this is effective for researchers comfortable with programming, it can be intimidating for those with limited coding experience. A natural next step would be to develop a user-friendly interface that integrates design, 3D model generation, and simulation into a single platform.

This would make the software more accessible to students and engineers, facilitating the adoption of origami metamaterials in broader mechanical design applications. A key limitation is the need for an open-source CAD engine with capabilities comparable to Fusion 360, including rendering and the export of STEP files for simulation and STL files for manufacturing. While the simulation pipeline is fully open source, CAD generation currently relies on Fusion 360 and proprietary slicing software such as Chitubox.

With our growing proficiency in CAD scripting, future work could explore translating the workflow to open-source platforms such as FreeCAD, enabling a fully open and self-contained design

ecosystem.

4.5.4 Enhanced Simulation and Validation

The current pipeline relies on CalculiX for static finite element analysis, providing a robust foundation but leaving room for enhancement.

One direction would be to integrate multiphysics simulations, including thermal, electromagnetic, or fluid-structure interaction capabilities. For example, origami-based reconfigurable antennas could operate across variable frequency ranges, and electromagnetic simulations would provide critical insights for such applications. Similarly, dynamic and frequency-response simulations could support vibration damping and impact studies.

Finally, introducing a feedback loop between design and simulation would enable data-driven optimization, where geometric parameters are automatically refined based on performance metrics extracted from simulations.

4.5.5 Manufacturing Integration and Material Considerations

The current workflow relies on the manufacturing resources available in Zhao's lab, which include FDM and SLA 3D printing. While these methods provide excellent design freedom, they also present limitations. FDM prints are porous and typically require additional coating for sealing, whereas SLA prints, although precise, can be brittle and sensitive to mechanical stress, heat, or radiation.

Future work could explore the use of composite materials such as Kevlar or Dyneema fibers for enhanced tensile strength, enabling extreme-environment applications, including aerospace or cryogenic structures. For medical applications, the availability of biocompatible resins already allows exploration of implantable or wearable devices.

Such developments would require more complex simulations and manufacturing processes but could significantly expand the software's relevance to high-performance applications.

4.5.6 Collaborative Research Platform

To accelerate progress in the field of origami metamaterials, a collaborative research platform could be established, enabling:

- Shared pattern libraries and open-source design repositories
- Standardized testing protocols and benchmarking datasets
- Integration with research databases and publication workflows
- Community-driven pattern development and validation

Such a platform could foster interdisciplinary collaboration and accelerate the translation of origami metamaterials from laboratory research to practical engineering solutions.

Conclusion

This thesis established an end-to-end workflow for the parametric design, simulation, and fabrication of origami metamaterials through the development of **ORIGAMI-STUDIO**. By combining semi-analytical and finite element simulations with SLA 3D printing, the framework bridges the gap between computational modeling and experimental validation.

A systematic exploration of crease geometries demonstrated that living hinges and curved folds significantly enhance folding predictability, stress localization, and energy absorption. These findings provide actionable design guidelines for future applications in deployable structures, soft robotics, and programmable mechanical metamaterials.

Beyond its immediate contributions, this work lays the foundation for more advanced generative design and AI-assisted workflows, ultimately enabling faster and more reliable development of origami-based mechanical systems.

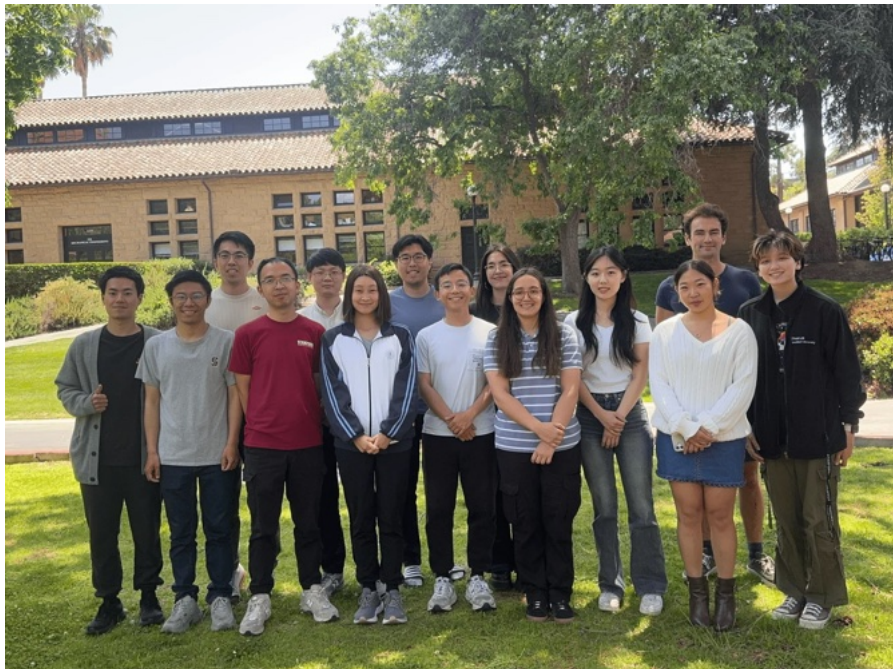
Acknowledgments

I would like to express my sincere gratitude to **Professor Renee Zhao** for her invaluable guidance, insightful discussions, and continuous support throughout this thesis. Her expertise in mechanical metamaterials and origami-inspired design has been a constant source of inspiration.

I am deeply thankful to **Yilong Chang** and **Sophie Leanza** for their patient mentorship and essential guidance during this project. They introduced me to the foundations of origami metamaterials and provided critical support in the development of **ORIGAMI-STUDIO**.

I am also grateful to the members of the **Zhao Lab** at Stanford for creating a stimulating, collaborative, and encouraging research environment.

Finally, I would like to extend my heartfelt appreciation to **Professor Selman Sakar** for his time, constructive feedback, and for kindly reviewing my master's thesis.



References

- [1] Khawlah Alabdouli, Israr Ud Din, Wesley Cantwell, Sean Swei, and Kamran Ahmed Khan. Multi-material additive manufacturing of yoshimura origami triangulated cylinder. *Progress in Additive Manufacturing*, 2025. doi:10.1007/s40964-025-01080-x.
- [2] Hugo de Souza Oliveira, Xin Li, Johannes Frey, and Edoardo Milana. Meta-ori: Monolithic meta-origami for nonlinear inflatable soft actuators. In *Proceedings of the ACTUATOR 2024; International Conference and Exhibition on New Actuator Systems and Applications*. VDE, 2024. To appear. URL: <https://www.softmachineslab.org/software>.
- [3] Lloyd Hamilton Donnell. Stability of thin-walled tubes under torsion. Technical Report NACA-TR-479, National Advisory Committee for Aeronautics (NACA), 1935. Accessed: 2025-07-24. URL: <https://ntrs.nasa.gov/api/citations/19930091553/downloads/19930091553.pdf>.
- [4] E. T. Filipov, T. Tachi, and G. H. Paulino. Bar and hinge models for scalable analysis of origami. *Journal of Applied Mechanics*, 81(6):061001, 2014. Accessed: 2025-07-24. URL: https://asmedigitalcollection.asme.org/appliedmechanics/article-pdf/81/6/061001/6435734/jam_081_06_061001.pdf, doi:10.1115/1.4026911.
- [5] Biruta Kresling. Folded and unfolded nature. In Koryo Miura et al., editor, *Proceedings of Origami Science and Art, Seian University of Art and Design, Otsu, Shiga, Japan, 1994*, volume 3, pages 93–108, 1997. Published 1997. URL: https://www.researchgate.net/publication/380100962_Biruta_KRESLING_Folded_and_Unfolded_Nature_In_Proc_Origami_Science_Art_Seian_University_of_Art_Design_Otsu_Shiga_Japan_1994_publ_1997_Koryo_Miura_et_al_eds_V3_93-108_12_figures.

- [6] Biruta Kresling. Natural twist buckling in shells: from the hawkmoth's bellows to the deployable kresling-pattern and cylindrical miura-ori. In *IASS-IACM 2008 Spanning Nano to Mega*, 2008. URL: https://www.researchgate.net/publication/382180201_Biruta_Kresling_2008_Natural_twist_buckling_in_shells_From_the_hawkmoth's_bellows_to_the_deployable_Kresling-pattern_and_cylindrical_Miura-ori_IASS-IACM_2008_pp_18-21.
- [7] Ting-Uei Lee, Xiaochen Yang, Jiayao Ma, Yan Chen, and Joseph M. Gattas. Elastic buckling shape control of thin-walled cylinder using pre-embedded curved-crease origami patterns. *International Journal of Mechanical Sciences*, 151:322–330, 2019. doi:10.1016/j.ijmecsci.2018.11.005.
- [8] K. Liu and G. H. Paulino. Nonlinear mechanics of non-rigid origami: an efficient computational approach. *Proceedings of the Royal Society A: Mathematical, Physical and Engineering Sciences*, 473(2206):20170348, 2017. doi:10.1098/rspa.2017.0348.
- [9] Diego Misseroni, Phanisri P. Pratapa, Ke Liu, Biruta Kresling, Yan Chen, Chiara Daraio, and Glaucio H. Paulino. Origami engineering. *Nature Reviews Methods Primers*, 4:40, 2024. doi:10.1038/s43586-024-00313-7.
- [10] Mark Schenk and Simon D. Guest. Nonlinear mechanics of thin-walled structures using origami-inspired folding patterns. *Proceedings of the Royal Society A: Mathematical, Physical and Engineering Sciences*, 469(2158), 2013. doi:10.1098/rspa.2012.0645.
- [11] Bo Wang, Shiyang Zhu, Peng Hao, Xiangju Bi, Kaifan Du, Bingquan Chen, Xiangtao Ma, and Yuh J. Chao. Buckling of quasi-perfect cylindrical shell under axial compression: A combined experimental and numerical investigation. *International Journal of Solids and Structures*, 130-131:232–247, 2018. doi:10.1016/j.ijsolstr.2017.09.029.
- [12] Yoshimaru Yoshimura. On the mechanism of buckling of a circular cylindrical shell under axial compression. Technical Report NACA-TM-1390, National Advisory Committee for Aeronautics (NACA), 1955. URL: <https://ntrs.nasa.gov/api/citations/19930093840/downloads/19930093840.pdf>.
- [13] Zirui Zhai, Lingling Wu, and Hanqing Jiang. Mechanical metamaterials based on origami and kirigami. *Applied Physics Reviews*, 8(4):041319, 2021. doi:10.1063/5.0051088.